RECONFIGURING SLIDING-MODE CONTROLLER FOR UNDERWATER VEHICLES

by

Ufuk Demirci

B.S. in E.E., Turkish Naval Academy, 1991

M.S. in Defense Technology, Boğaziçi University, 1998

Submitted to the Institute for Graduate Studies in
Science and Engineering in partial fulfillment of
the requirements for the degree of
Doctor of Philosophy

Graduate Program in Electrical and Electronics Engineering

Boğaziçi University

2004

ACKNOWLEDGMENTS

I would like to express my sincere gratitude to Professor Feza Kerestecioğlu for his continuous support, invaluable guidance and helps during the preparation of this dissertation. I would like to mention his patience, giving me inspiration and hope when I was in deep depression. It was a pleasure to work with him as my mentor since the beginning of my master studies in 1996.

I am honored by the presence of Professors Kadri Özçaldıran, Kemal Cılız, Emre Köse and Kemalettin Erbatur in the dissertation jury. I also express my gratitude for reading the dissertation and for their comments and suggestions. I'm indebted for valuable guidance and comments of Professors Yağmur Denizhan, Kadri Özçaldıran and Emre Köse during dissertation studies.

I also would like to express my gratitude to all my former instructors for constituting the necessary background for completing this dissertation and my former and present superiors, especially, Lt.Cdr. Cem ÖNEY (retired), Dr.Lt.Cdr. Doğan Özdemir, Cdr. İbrahim Aksu and Captain Sami Örgüç who let me feed myself with knowledge and all my former and present subordinates especially, MCPO Bahadır Özgün who worked hard to make up for my absence during PhD studies. I would also like to thank Nur Başürün for her extra assistance and easing the problems as I was in Ankara.

I would like to express my sincere gratitude to my second home Turkish Navy for giving me opportunity to have an education and giving me a break in Naval Academy for a year as a lecturer to complete my dissertation.

I am thankful to my family as they always believed that I would make it. Finally, I would like to express my deepest thanks and affection to my wife Helene for her endless patience, support and love, and to our children Ela and Teoman for their unrestrained devotion that I've always felt during this study. I would like to mention my wife's convincing me to continue and complete my studies.

ABSTRACT

RECONFIGURING SLIDING-MODE CONTROLLER FOR UNDERWATER VEHICLES

The challenging control problem of underwater vehicles is addressed in this study under excessive sea wave disturbances at shallow submerged operation. The systems are becoming more and more complex with the effect of rapid technological developments. These complex systems require fault tolerant control systems in order to accommodate with the uncertainties caused by faults or environmental changes. In this doctoral dissertation, a novel re-configuring controller is proposed based on sliding mode methodology for fault or disturbance tolerant control. Re-configuring control with sliding mode technique annuls the unwanted effects of system uncertainties caused by faults and environmental effects and avoids the chattering by increasing the robustness of the controller when it is necessary. As a result acceptable performance is obtained in case of system uncertainties and the chattering phenomenon is eliminated for the nominal system situation.

ÖZET

SUALTI ARAÇLARI İÇİN YENİDEN YAPILANABİLİR KAYAR KİPLİ DENETLEYİCİ

Bu çalışmada sığ suda harekat icra eden sualtı araçlarının aşırı deniz dalga etkileri gibi zor şartlar altında denetimi problemi incelenmiştir. Hızlı teknolojik gelişmelerin sonucunda sistemler gittikçe daha karmaşık hale gelmektedirler. Bu karmaşık sistemler arızalardan ve çevresel etkenlerden kaynaklanan sistem belirsizliklerinden etkilenmemek için arızaya müsamahalı denetime ihtiyaç duymaktadırlar. Bu doktora tezinde, arızaya müsamahalı denetim için kayar kip tekniğini temel alan yeni bir yeniden yapılanabilir denetleyici önerilmiştir. Kayar kipli teknikle yeniden yapılanabilir denetim arızalardan ve çevresel etkilerden kaynaklanan sistem belirsizliklerinin etkilerini sıfırlar ve sadece gerektiğinde denetleyicinin gürbüzlüğünü artırarak çatırtıdan kaçınmayı sağlar. Sonuç olarak sistem belirsizlikleri durumunda kabul edilebilir bir performans sağlanır ve nominal sistem durumunda çatırtı olayı ortadan kaldırılmış olur.

TABLE OF CONTENTS

LIST OF FIGURES

LIST OF TABLES

LIST OF SYMBOLS

$\mathbf{A}$	System matrix
$\mathbf{A}_{fault}$	Faulty system matrix
$\Delta\mathbf{A}$	Uncertainty matrix for system matrix
$\mathbf{B}$	Input matrix
$\mathbf{B}_{fault}$	Faulty input matrix
$\Delta\mathbf{B}$	Uncertainty matrix for input matrix
δB	Actual bow plane command
δB_c	Commanded bow hydroplane deflection
b	Input gain
$\mathbf{C}$	Output matrix
$\mathbf{d}$	Unknown input vector
$\mathbf{E}$	Distribution vector
$\mathbf{e}$	State estimation error
$\mathbf{F}$	Observer matrix for UIO/Uncertainty matrix for model mismatch
F_{li}	Force due to attenuated static head
$\mathbf{F}$	Fault vector
f	Unknown dynamics
$\mathbf{f}_a$	Actuator fault vector
$\mathbf{f}_s$	Sensor fault vector
G_c	Closed loop transfer function
g	Gravitational acceleration
$\mathbf{H}$	Observer matrix for UIO
H_s	Significant wave height
h	Depth value
$\mathbf{K}$	Observer matrix for UIO
K	Gain
k	Gain
k_{fault}	Faulty plant gain

k_{nom}	Nominal plant gain
$\mathbf{L}$	Observer gain vector/matrix
L	Length of the submarine
$\mathbf{M}$	Inertia matrix
M_{wave}	Instantaneous moment in pitch
M_e	Instantaneous auxiliary tank content
m	Weight of the submarine
Q	Pitch rate
$\mathbf{R}$	Uncertainty distribution matrix
$\mathbf{r}$	Residual vector
$\mathbf{r}_y$	Output residual vector
$\mathbf{r}_\theta$	System parameter residual vector
S	Sea spectrum
δS	Actual stern plane command
δS_c	Commanded stern hydroplane deflection
s	Sliding surface
$\mathbf{T}$	Observer matrix for UIO
$\mathbf{u}$	Control input vector
u_{eq}	Equivalent control
V	Wind speed
v	Instantaneous sea surface wave elevation
w	Velocity of the submarine along z axis
$\mathbf{x}$	State vector
x_d	Desired trajectory
$\hat{\mathbf{x}}$	State estimation vector
$\tilde{x}$	Tracking error
$\mathbf{y}$	System output vector
$\hat{\mathbf{y}}$	Estimate of the system output vector
Z_{wave}	Instantaneous force in heave due to the sea waves
$\mathbf{z}$	Observer state vector

ϕ	Heading of the submarine
η	Positive scalar
φ	Threshold value
λ	Positive scalar
ρ	Mass density of sea water
θ	System parameter vector
$\hat{\theta}$	Estimate of the system parameter vector
ω	Wave frequency

AUV	Autonomous underwater vehicle
DOF	Degree of freedom
DOS	Dedicated observer scheme
FD	Fault detection
FI	Fault isolation
FDI	Fault detection and isolation
MIMO	Multi-input-multi-output
NATO	North atlantic treaty organization
ROV	Remotely operated vehicle
SISO	Single-input-single-output

1. INTRODUCTION

Control of underwater vehicles for shallow water operations is a challenging problem under the excessive sea wave effects. In this thesis, the control of underwater vehicles is addressed with a proposed reconfiguring controller based on the sliding-mode scheme.

1.1. Underwater Vehicle Control

Underwater vehicles are modelled with six degree of freedom (DOF) nonlinear equations. They are controlled in depth and steering directions. Sea waves have adverse effects on underwater vehicles at shallow submerged operation. Sea waves tend to bring the underwater vehicles towards the surface of the sea with an effect that is called suction force. On the other hand, due to suction force and sea wave currents, steeringcontrol is also a challenging problem for underwater vehicles at shallow submerged operation. In this thesis, depth and pitch angle controls of underwater vehicles under excessive sea wave disturbances are investigated.

In fact, there are both commercial and military applications of underwater vehicles and therefore, many researchers addressed the control of underwater vehicles with different control methods. But not many of them addressed the challenging depth control of underwater vehicles under excessive sea wave disturbances.

One of the controller solution for shallow submerged operation of underwater vehicles is proposed in [1]. A multivariable (2x2) H_∞-controller is designed in this study for depth control of a submarine under sea wave disturbances. A linearised model of a submarine is used for the controller design. It is observed that designed H_∞-controller causes bow hydroplane actuator to saturate which in return, caused overall system to be unstable. In short the designed controller cannot cope with sea wave disturbances.

Another implementation is the depth control of a submarine [2] under sea wave disturbances. The gain scheduling approach is used and different gain sets for a stochastic

controller is a priori calculated. Steady-state estimator gains corresponding to different wave heights for different sea states are also calculated and used for estimating the real wave height by switching the gain sets. This approach requires excessive computations at the design phase for all possible sea states and in particular significant wave heights.

There are a variety of control methods which are implemented on underwater vehicles without considering sea wave disturbances. Among them, sliding-mode control [3] scheme is commonly used as it is robust to uncertainties caused by model mismatch or environmental disturbances as a passive reconfiguring controller when the boundary of the uncertainty is known. Therefore, sliding-mode control is a suitable candidate that can be implemented for the control of underwater vehicles, which, has a challenging problem to be modeled due to 6 degree of freedom (DOF) coupled nonlinear differential equations. Model mismatch is unavoidable, as analytical methods for obtaining hydrodynamic coefficients of an underwater vehicle cannot give precise results. They are also operated under changing sea conditions; therefore, uncertainties are also unavoidable due environmental conditions.

Applications of sliding-mode controllers briefly reviewed below are used for steering, depth and speed control of underwater vehicles without considering faults or operation in excessive disturbance environment.

One of the first underwater vehicle applications of sliding-mode controllers is the JASON remotely operated vehicle (ROV) [4]. A sliding-mode controller for JASON ROV is used for the vehicle to follow a pre-defined trajectory in a test pool. It is shown that the performance of the controller increases as model uncertainty decreases. Different models are used to show the increase of the performance for trajectory following task when the model mismatch level is decreased.

A different application of sliding mode control method is combining adaptive control methods with sliding-mode control method [5]. In this application, the problem of controlling an Autonomous Underwater Vehicle (AUV) in a diving maneuver is implemented. The implemented controller is called as adaptive sliding mode controller and the controller is based on a reduced order linear model of AUV based on the dominant

poles of the plant. The estimates of the parameters of the model dynamics are used for the equivalent control part of the controller in a way similar to indirect adaptive model-reference control method [6].

Another application of sliding mode controller is the multivariable sliding mode controller [7] based on state feedback which is operated for the combined speed, steering and diving response of a slow forward speed AUV. The so-called waypoint following problem is achieved by compensating the influence of speed, modeling nonlinearity and uncertainty. A linearized model of AUV is used for the equivalent control part of the controller. This part is obtained by means of linear feedback regulator. Separate autopilots are used for separate subsystems; speed, steering and diving systems. It is assumed that mentioned subsystems are not coupled.

In this study sliding-mode controller scheme is used as a baseline controller for the nominal plant and possible reconfiguration approaches for sliding-mode control scheme is investigated in case of faults or operating under excessive environmental disturbances. Therefore, next Section introduces control reconfiguration which is used when the controllers designed for nominal cases cannot cope with faults and disturbances. Reconfiguring controllers either updates in an adaptive manner the controller coefficients or reconfigure the structure of the controller.

1.2. Control Reconfiguration

Autonomous control reconfiguration [8] is a very important issue. Nowadays, the engineering systems are becoming more and more complex. These complex systems require robustness in order to guarantee continuous operation in case of uncertainties caused by faults and environmental changes.

Fault tolerant controllers have the ability to tolerate the faulty situation of a system dynamics and be able to continue operation with a degraded performance [9]. Appropriate fault handling provides continuous operation. In order to handle faulty situations of systems, the fault information is required to be detected and isolated. Therefore, a variety

of fault detection and isolation schemes are used for the fault detection and isolation (FDI) block in Figure 1.1.

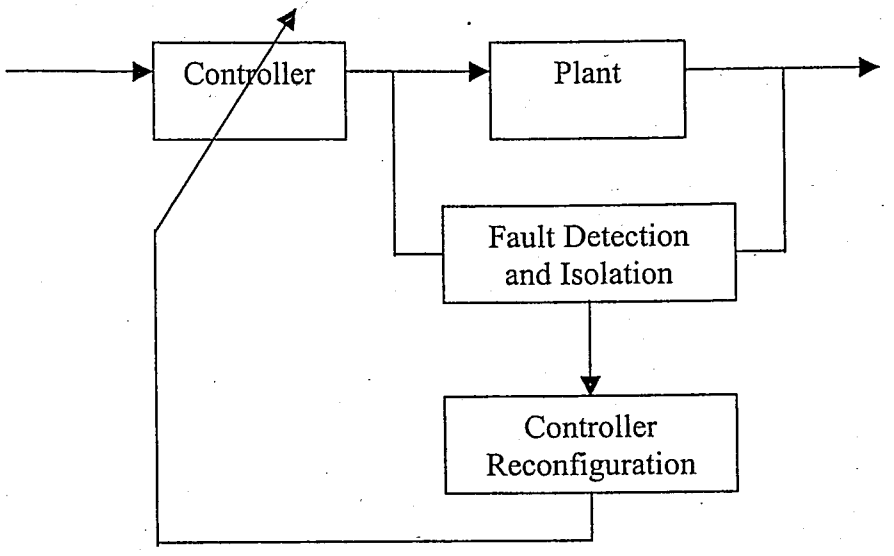

Figure 1.1. Fault tolerant controller scheme

Controller reconfiguration is provided based on the fault information and the controller block is updated in order to cope with faulty situation. Controller reconfiguration block in Figure 1.1 will be described in detail later.

Fault tolerant control is vital for future applications of underwater vehicles. Autonomous control of underwater vehicles for mine detection and classification operations at littoral waters is the strategic mission of North Atlantic Treaty Organization (NATO) Navies. Unmanned mine operations are essential for Navies due to public pressure for not using manned mine hunting and sweeping vessels [10]. Therefore, underwater vehicles are required to be operating autonomously for long periods.

Fault tolerant control is primary requirement of navies in order to have reliable vehicles, which will be operating effectively in case of faults or harsh environmental conditions of littoral water operations. Navies are planned to have such an autonomous mine detection and classification vehicle in next decade. Therefore, it is expected that there will be increasing number of studies supported by NATO Navies will be exponentially increasing in the upcoming a couple of years. The proposed scheme is a contribution for

the requirement defined above in order to have a fault tolerant controller scheme which can be used both for in case of faults of vehicles and harsh environmental conditions of sea when it is not possible or feasible to terminate the operation and fix the fault or change the unprecedented behavior of sea.

Reconfiguration methods for controllers are shown in Figure 1.2 [11]. There are two main approaches, namely, active and passive reconfigurable control methods.

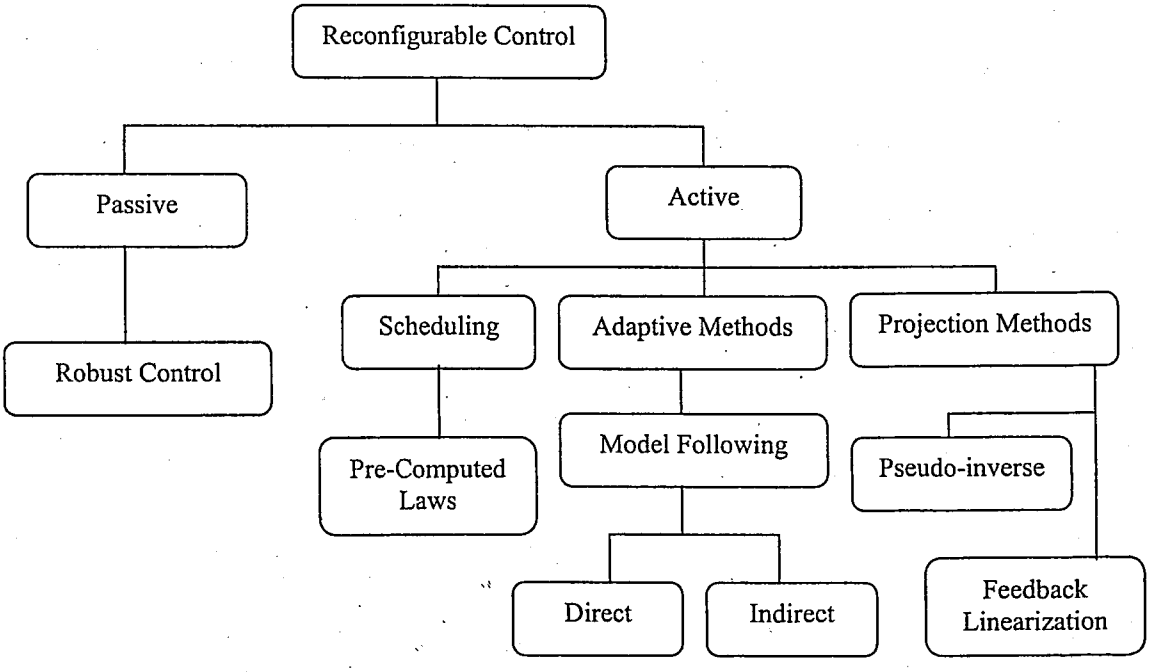

Figure 1.2. The tree diagram of reconfigurable control methods [11]

The passive approaches to control reconfiguration require a robust controller, which is designed off-line in order to achieve robustness against disturbances and possible faults. Once the robust controller is designed to accommodate possible faults, which might change the system parameters then it is not possible to reconfigure the controller on-line in case of unpredicted faults or disturbances. The use of a robust control technique alone as a passive reconfiguring controller for fault accommodation can be quite risky. If disturbance and modeling uncertainties are present in the system that are not accounted for during the (off-line) design of the robust controller, then they might insert adverse effects on the system. Also nearly all passive control re-configuration designs in [12, 13] do not challenge the robustness problem and do not consider the smaller or incipient effects of disturbances which may happen in real applications, but only consider large effects.

There are also a great variety of active control re-configuration techniques. Control law re-scheduling [14] is implemented mainly for flight control systems. This method requires the knowledge of the fault or disturbance characteristics and their effects on system dynamics. In return, different sets of control gains or parameters can be calculated a priori considering possible changes in dynamics. In many cases, an effective disturbance monitoring mechanism is required in order to extract uncertainty information accurately. By doing so, the correct control schedule can be implemented without any operator supervision. The main drawback of this method is the requirement of precise fault or disturbance information otherwise an incorrect re-scheduling may degrade the system performance.

Another active reconfiguration method is pseudo-inverse method [15]. The feedback gain is updated in a way to approximate the nominal system performance in case of a priori known possible faults or disturbances. Gain sets are designed for all possible faults and disturbances. No fault detection or disturbance monitoring mechanism is required, but the stability and performance of the system in case of an unanticipated fault or disturbance cannot be guaranteed.

Model following as an active reconfigurable control technique is implemented for many applications with many different adaptive methods in [16, 17 18]. For example, adaptive reconfiguration via model following method uses the estimated system parameters for updating the controller scheme in case of disturbances [19]. The problem with this method is the difficulty in estimating system parameters accurately. In some cases, the input signals for the estimators are not persistently exciting enough. In return, the updated controller parameters cannot provide the desired response.

1.3. Fault Detection and Isolation

FDI is a widely investigated issue and there exist a variety of FDI approaches in the literature. Main approaches are observer based, parity relations and filtering techniques. The detailed surveys about FDI schemes are given in [20, 21, 22, 23, 24, 25].

Observer based FDI methods are explained further in detail in this dissertation. Fault information is detected by means of residuals generated by comparing actual plant dynamics with estimated ones. If a priori information is available about possible faults, which might occur in system, actuators or sensors, then a pre-defined threshold is defined. If the residual generated exceeds the pre-defined threshold value, then, the operator or the controller is warned about the fault. If the controller is a reconfiguring controller in order to provide fault tolerant control, then, mentioned fault information is fed to controller reconfiguration block in Figure 1.1.

1.4. Contribution and Outline of the Dissertation

Challenging problem of underwater vehicles under excessive sea wave disturbances is investigated and two approaches are proposed in this study which have some advantages with respect to other proposed controllers. Proposed approaches combines fault detection and isolation methods with sliding-mode control scheme in order to obtain an active reconfiguring controller for the challenging control problem of underwater vehicles under excessive sea wave disturbances at shallow submerged operation.

The proposed approach is an active (on-line) control re-configuration scheme, which uses the well known robust sliding-mode control method as the baseline controller of the nominal plant. The sliding mode controller method is used as a passive baseline controller for slowly developing so-called incipient faults. Sliding-mode controller gain vector is reconfigured when a fault or an uncertainty is monitored by an observer based FDI scheme. A disturbance or fault distribution information is extracted from plant dynamics by using observers. This disturbance distribution information is used to adjust the robustness of the sliding mode controller to annul the unwanted effects of uncertainties on tracking performance. No pre-calculations except those required for the nominal plant are involved, nor are a priori information on fault or disturbance required.

In case of unanticipated changes in system dynamics, which can be processed as additive disturbances, the robustness of the sliding-mode controller is increased using disturbance distribution information. Chattering, the main drawback of the sliding-mode controller is eliminated by using a soft nonlinear switching function for the nominal plant.

The chattering is almost unavoidable for a plant subject to disturbances as the control action should be increased extensively to compensate unwanted effects. But the stability of the on-line reconfigured controller is guaranteed due to the nature of baseline sliding mode controller in case of excessive disturbances as well as disturbance-free case. A Lyapunov function is defined in terms of a sliding manifold and along which the stability is guaranteed for sliding-mode controllers [26].

Sliding mode control scheme has been recently used for reconfiguration purposes by [27] and [28]. McGookin (2003) describes the use of sliding-mode controller as a passive baseline controller. However, this method provides tolerance only for certain sensor faults of a submarine model. On the other hand, Yen and Ho (2000) implemented a sliding-mode controller scheme for a SISO system in a way that the faults or uncertainties are detected by means of a neural network observer. The robustness of the sliding mode controller is increased without taking care of the direction of the uncertainty. In the meantime neural network model is trained for the faulty system, which causes a great deal of computational burden. In our solution a generalized MIMO system is used and the disturbance distribution vector directions are also extracted from the uncertainty information.

In this study, a new control mechanism is proposed with active reconfiguration, which uses sliding mode control technique as the baseline controller [29]. The uncertainties caused by unanticipated faults and disturbances are extracted by means of observers. The controller is reconfigured with respect to uncertainty information and the stability of the controller is guaranteed by robustness property of sliding-mode control method. By means of its robustness property, sliding-mode control can compensate minor disturbances. The proposed control scheme can also cope with larger disturbances by updating itself with respect to on-line monitored uncertainty information. The robustness of the sliding mode controller is updated only using the disturbance distribution vector direction without increasing the computational burden involved appreciably. It is believed that this proposed fault tolerant controller idea which bounds active and passive reconfiguration control scheme contributes to this area of research.

In order to address these objectives, this dissertation is organized in the following way:

In the next chapter, MIMO submarine model together with environmental effects are examined. A generalized 6 DOF nonlinear equations of motions together with earth and body fixed reference frames are also addressed in this chapter. MIMO submarine model for the depth and pitch angle control of a submarine under sea wave effects are examined in this chapter. Sea wave model is derived in detail together with effects on shallow submerged submarines. Sea wave effects as disturbances are addressed and the effects of sea waves for a submarine operating near the surface are investigated. Proposed reconfiguring controller is implemented for the submarine model together with sea wave effects.

Chapter 3 addressed to different important facts about residual generation and evaluation. Different fault detection and isolation (FDI) approaches are also mentioned in this chapter. Theoretical information regarding fault detection (FD) scheme is supported with case-study simulations.

In Chapter 4, the basics of the sliding-mode control and proposed control approach with sliding-mode control scheme are examined in detail. The necessity of the proposed approach and the requirement for a reconfiguring sliding mode controller is explained in detail with a SISO linear model. Fault and disturbance extraction is addressed and the application of the proposed scheme for multi-input-multi-output (MIMO) linear systems together with simulation studies is also shown in this chapter. The implementation of the proposed scheme for MIMO linear systems is investigated in detail with two approaches. The first one is the performance of the controller when the extracted disturbance distribution information is used to update the gain vector in the corrective control part of the sliding mode controller and the second one is the performance of the controller when the extracted disturbance distribution information is inserted into equivalent control part of the sliding mode controller. Detailed stability analysis with proposed controller schemes are also investigated in detail in this part.

In the Chapter 5 simulation results for different sea states are illustrated for the submarine model at shallow water operation. It is observed that standard sliding-mode controller scheme cannot perform the trajectory control task of the submarine for depth

control when there exists excessive disturbances caused by sea state 6 situation. However, proposed novel approach shows satisfactory results for different sea state situations.

In the Chapter 6, concluding remarks and recommendations are given for future work.

2. MODELLING OF SUBMARINES AND SEA WAVE EFFECTS

2.1. Shallow Submerged Submarine Operation

In this chapter, a model for submarines at shallow submergence under sea wave disturbances is investigated. The model will be used in order to illustrate the effectiveness of implementation of observer based fault detection (FD) methods with reconfiguring control. Shallow water operation has vital importance for conventional submarines to use their periscope and charge batteries while cruising in diesel-engine mode. However the depth control becomes more difficult when the vessel is close to the surface due to adverse effects of sea conditions. The wave forces try to pull the submarine to the surface at shallow submerged operation. Because of sea wave effects it is very difficult to operate the submarine manually for long period of operation time. Therefore a depth controller for shallow submerged operation is vital in order to avoid submarine crew to be exhausted.

The vessel at shallow-submerged position is effected by sea waves rather than currents in the sea that is neglected in this study. The vehicle in this dissertation [2] has two control surfaces, namely, the bow and stern planes. Also, the content of the trim tanks is used as a constant control input. But the content of the trim tanks is assumed to be defined and implemented prior to control activity. The depth and pitch angle measurements are performed by a hydrostatic pressure sensor and a gyroscopic system, respectively. The vehicle is assumed to be at shallow submergence and has initially constant low speed forward motion. The vehicle is also assumed to be stable in roll axis and no control activity required for roll motion. Therefore, the yaw motion which is controlled by the rudder is uncoupled from the pitch motion.

The submarine beneath the sea waves is subject to sea forces and moments. These forces are composed of first and second order parts of sinusoidal wave patterns. The first order forces tend to cancel each other along the hull of the vehicle and can be neglected for the controller design. Second order part of the wave effect tends to pull the vehicle towards

to surface. The latter one becomes smaller as the depth increases. This is called *suction force* [30].

Equations of motion of a submarine consist of nonlinear differential equations. These equations are derived in six degrees of freedom [30]. Since the control action is not performed for yaw and roll axes, the pitch and heave equations are used for the controller design. For working with a linear model is much simpler than a nonlinear one, the nonlinear equations of the submarine for the pitch and heave axes to be linearized around an equilibrium point.

The adverse effects of the sea waves are modeled to include in the overall submarine model for a more realistic controller design. Sea states can be defined with respect to sea wave heights from sea state 0 (calm –glassy-) up to 9 (phenomenal) [30]. In this study, the sea states from 1 (calm –rippled-) and 6 (very rough) are modeled in order to investigate the control performance for different sea wave heights as most vessels are designed to be robust up to sea state 6.

2.2. Submarine Dynamics

A nonlinear 6 degree-of-freedom (DOF) hydrodynamic model of a generic underwater vehicle [30], [31] can be used to describe necessary dynamic information which describes the motion of the submarine relative to its body-fixed reference frame and earth-fixed reference frame. The model is derived from two reference frames; therefore, there are two parts of the model of an underwater vehicle; namely,

- Kinetic (body-fixed hydrodynamic forces),
- Kinematics (represents transformation from body to earth fixed reference frame)

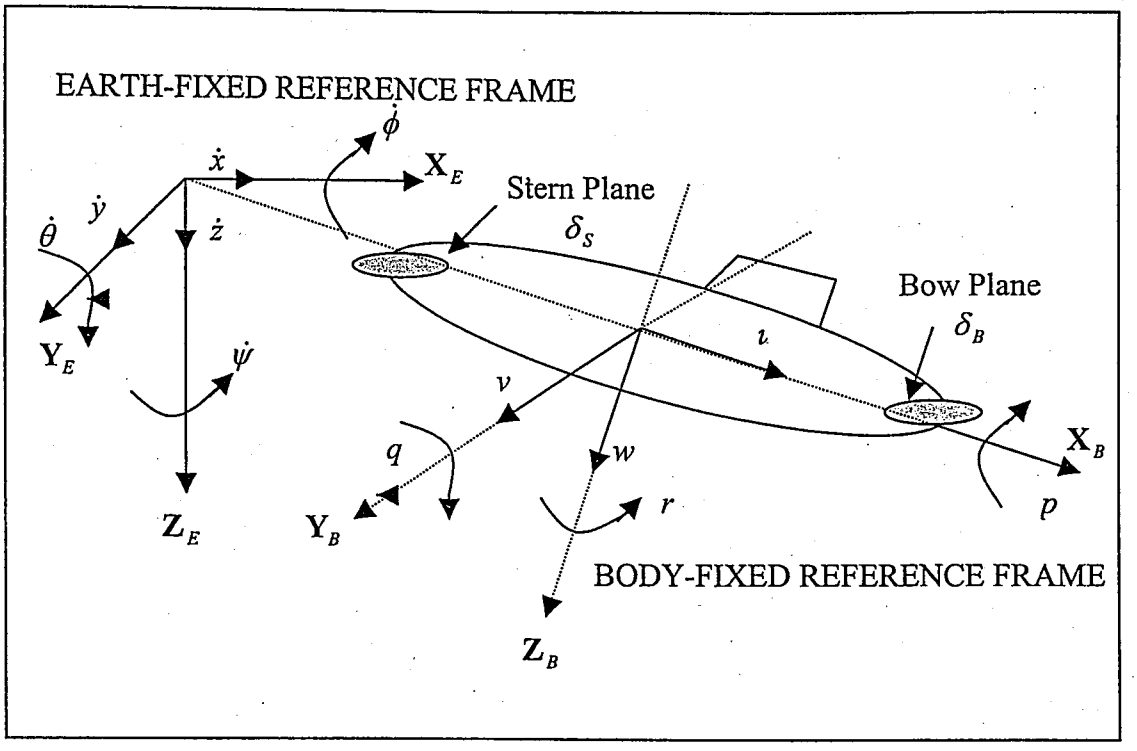

Figure 2.1. Submarine reference frames [27]

The kinetic and kinematic equations form the 6 DOF motion of a submarine. The notation used for submarines are listed in Table 2.1, and the variables are depicted in Figure 2.1.

Table 2.1. Notation used for submarines [30]

DOF		Forces and Moments	Linear and Angular Velocities	Positions and Euler Angles
1	motions in the x-direction (surge)	X	U	x
2	motions in the y-direction (sway)	Y	v	y
3	motions in the z-direction (heave)	Z	w	z
4	rotation about the x-axis (roll)	K	p	ϕ
5	rotation about the y-axis (pitch)	M	q	θ
6	rotation about the z-axis (yaw)	N	R	ψ

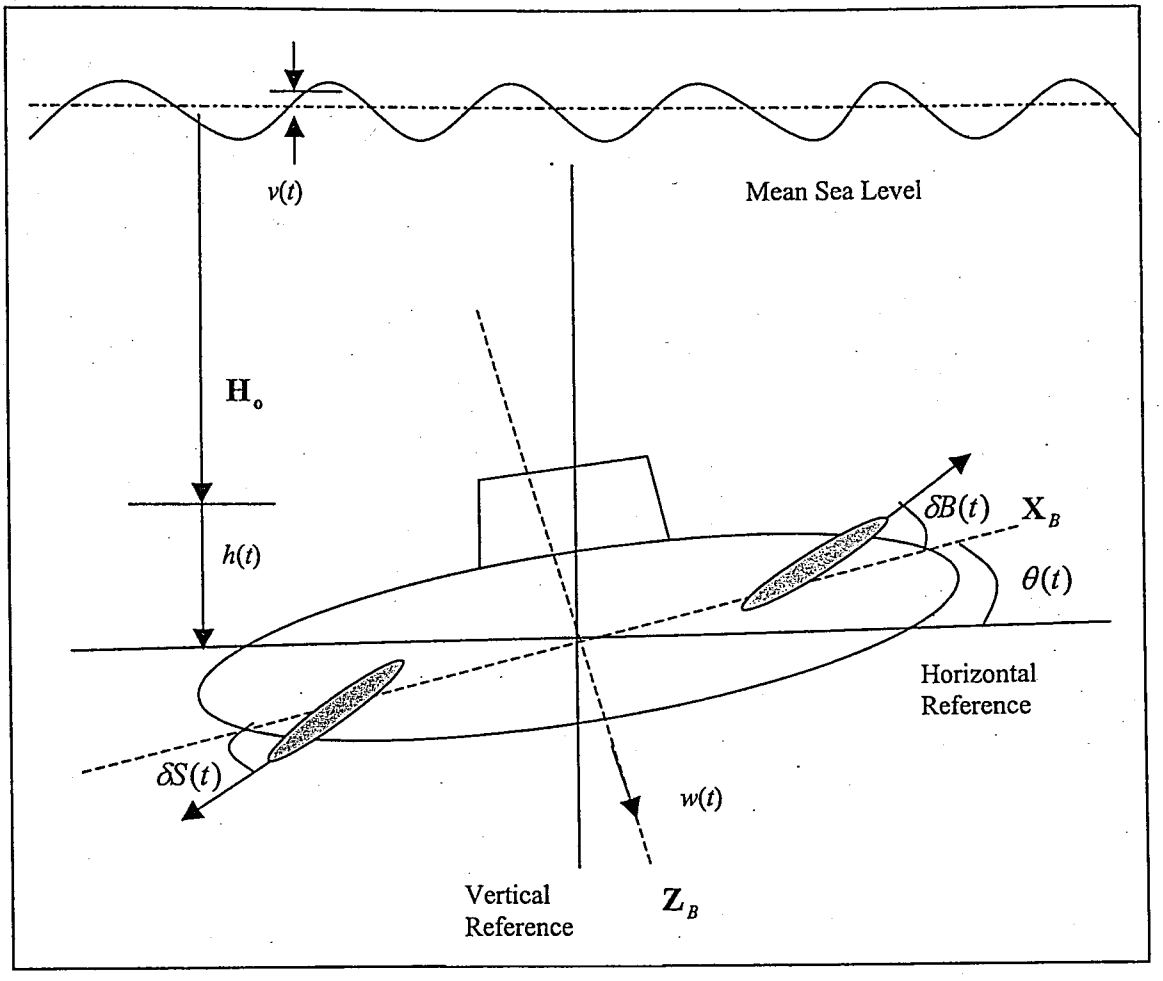

Figure 2.2. Depth deviation of a trimmed submarine [2]

Six DOF nonlinear dynamic equations of a submarine can be expressed in the following general form [30]:

$$\mathbf{M}\dot{\upsilon} + \mathbf{C}(\upsilon)\upsilon + \mathbf{D}(\upsilon)\upsilon + \mathbf{g}(\eta) = \tau\,, \tag{2.1}$$

where

$\mathbf{M}$ = inertia matrix (including added mass)

$\mathbf{C}(\upsilon)$ = matrix of coriolis and centripetal terms (including added mass)

$\mathbf{D}(\upsilon)$ = damping matrix

$\mathbf{g}(\eta)$ = vector of gravitational forces and moments

τ = vector of control inputs

The variables associated with the motion of a submarine along the pitch and heave axes are shown in Figure 2.2 with respect to its body-fixed reference plane.

The derivation of submarine model used in this dissertation is investigated in detail in [2]. Therefore, only heave and pitch axis equations of motion are investigated in this part.

Equation of motion along z-axis (normal force) is given

$$\dot{w}(t) = \frac{Z_w' U}{Lm_3'} w(t) + \frac{1}{m_3'}(Z_{\dot{\theta}}' + m')U\dot{\theta}(t) + \frac{Z_{\ddot{\theta}}' L}{m_3'}\ddot{\theta}(t) + \frac{Z_{\delta B}' U^2}{Lm_3'}\delta B(t) + \frac{Z_{\delta S}' U^2}{Lm_3'}\delta S(t) + \frac{2}{\rho L^3 m_3'} Z_{wave}(t) + W_e(t)\cos\theta\cos\phi\frac{2}{\rho L^3 m_3'} \tag{2.2}$$

where w(t) is the velocity of the submarine along z axis, θ is the pitch angle and h is the depth value, ρ is the mass density of sea water, L is the length and m is the weight of the submarine, U is the forward speed of the submarine , δB is the bow plane command and δS is the stern plane command. Z_{wave} is the instantaneous force in heave due to the sea waves, $m' = 2m/\rho L^3$, $m_3' = m' - Z_{\dot{w}}'$ and $W_e(t) = M_e(t)\cdot g$. Here $M_e(t)$ is the instantaneous auxiliary tank content in slugs and g is the gravitational acceleration.

Equation of motion along y-axis (Pitching Moment) is given

$$\ddot{\theta}(t) = \frac{M_{\dot{w}}'}{LI_2'}\dot{w}(t)0 + \frac{M_w' U}{L^2 I_2'} w(t) + \frac{M_{\dot{\theta}}' U}{LI_2'}\dot{\theta}(t) + + \frac{M_{\delta B}' U^2}{L^2 I_2'}\delta B(t) + \frac{M_{\delta S}' U^2}{L^2 I_2'}\delta S(t) + \frac{2mg(z_G - z_B)}{\rho L^5 I_2'}\theta(t) + \frac{M_{wave}(t)}{\frac{\rho}{2}L^5 I_2'} \tag{2.3}$$

where z_G and z_B are the vehicle dimensions, M_{wave} is the instantaneous moment in pitch due to the sea waves, $I_2' = I_{G_y}' - M_{\ddot{\theta}}'$ and I_{G_y}' is the moment of inertia about the center of gravity. All primed quantities in (2.2) and (2.3) are hydrodynamic coefficients. Hydrodynamic coefficients are given in Appendix-A.

By substituting the hydrodynamic coefficients and other values which are given in [2], and substituting equations (2.2) and (2.3) to each other, we obtain

$$\begin{aligned}\dot{w}(t) &= -2.45313\text{x}10^{-2}w(t) + 1.5174Q(t) + 4.6192185\text{x}10^{-2}\delta B(t) - 7.9592688\text{x}10^{-2}\delta S(t) \\ &\quad + 1.62\text{x}10^{-2}\theta(t) - 2.2\text{x}10^{-9}M_{wave}(t) + 3.06\text{x}10^{-6}Z_{wave}(t) + 9.8\text{x}10^{-5}M_{e_{aux}}, \\ \dot{Q}(t) &= 3.3720\text{x}10^{-4}w(t) - 7.71345\text{x}10^{-2}Q(t) + 4.79688\text{x}10^{-4}\delta B(t) - 2.184535\text{x}10^{-3}\delta S(t) \\ &\quad - 0.003975\theta(t) + 5.42\text{x}10^{-10}M_{wave}(t) - 2.20\text{x}10^{-9}Z_{wave}(t) - 7.14\text{x}10^{-8}M_{e_{aux}}\end{aligned} \tag{2.4}$$

where $\dot{Q}(t) = \ddot{\theta}(t)$ and $U = 8.43$ ft/sec.

These are the state equations of the submarine dynamics; the state variables are being the pitch velocity and heave velocity. From (2.4), the state-space model of the submarine dynamics can be written as

$$\dot{\mathbf{x}}(t) = \mathbf{A}\mathbf{x}(t) + \mathbf{B}\mathbf{u}(t) + \mathbf{R}\mathbf{d}(t) \tag{2.5}$$

with

$$\begin{aligned}\mathbf{x}(t) &= \left[w(t), Q(t), \theta(t)\right]^T, \\ \mathbf{u}(t) &= \left[\delta B(t), \delta S(t), M_{e_{aux}}\right]^T, \\ \mathbf{d}(t) &= \left[Z_{wave}(t), M_{wave}(t)\right]^T.\end{aligned}$$

where $\mathbf{x}(t) \in \Re^n$ is the state vector, $\mathbf{u}(t) \in \Re^r$ is the control input vector and $\mathbf{y}(t) \in \Re^m$ is the measurement vector, and the values of **A**, **B** are obvious from (2.4). The vector

$\mathbf{d}(t) \in \Re^h$ is the disturbance vector representing sea force component along the z-axis and moment of sea waves about y-axis. The matrix **R** is the disturbance distribution matrix.

2.3. Sea Model

The submarine beneath the sea waves is subject to sea forces and moments. These forces are composed of first and second order parts of sinusoidal wave patterns [32]. The first order forces are proportional and periodic. Second order forces are proportional to the square of the wave component and tend to pull the vehicle towards to surface. The latter one becomes smaller as the depth increases. The adverse effects of the sea waves are modeled to include in the overall submarine model for a more realistic controller design. The sea model given in this paper is the one accepted in International Towing Tank Conference (ITTC) [2, 30].

A storm at sea starts with high frequencies of wavelets generated due to wind. A fully developed sea is created by a storm which has been blowing for a long time. Low frequency decaying sea forms long waves with a wave spectrum having a low modal frequency after the storm stopped or decreased its effect [30]. From analysis of wave spectra in the North Atlantic Ocean, a wave spectral formulation for fully developed wind-generated seas is given by the equation [30],

$$S(\omega) = A\omega^{-5} \exp(-B\omega^{-4}) \quad (m^2 s) \tag{2.6}$$

where, ω is the wave frequency in rad/sec.,

$$A = 8.1 \times 10^{-3} g^2 \text{ and } B = 0.74(\frac{g}{V})^4$$

Here V is the wind speed at a height of 19.4 m over the sea surface and g is the gravitational acceleration. Wind speed and *significant wave height*[1] H_s can be related as,

[1] Mean of the one-third highest waves, denoted by $H_{1/3}$ in some text books.

$$H_s = 0.21\frac{V^2}{g} \tag{2.7}$$

The sea spectrum expression in terms of the significant wave height can be obtained by inserting (2.7) into (2.6) as

$$S(\omega) = 8.1\times10^{-3}\omega^{-5}\exp(-\frac{3.11}{H^2{}_s}\omega^{-4}) \quad (m^2 s) \tag{2.8}$$

The sea state definition with respect to significant wave height is shown in Table 2.2.

Table 2.2. Description of sea states [33]

Sea State Code	Description of Sea	Significant Wave Height (m)
0	Calm (glassy)	0
1	Calm (rippled)	0-0.1
2	Smooth	0.1-0.5
3	(wavelets)	0.5-1.25
4	Slight	1.25-2.5
5	Moderate	2.5-2.0
6	Rough	2.0-6.0
	Very Rough	

The wave spectrums for different significant wave heights can be seen in Figure 2.3.

The frequency range of sea wave components can be divided into N bands of width $\Delta\omega$. Sea component can be approximated by a sinusoidal function with the center frequency of each band and the instantaneous wave height for this component can be calculated as [2, 34],

$$v_i(t) = A_i \sin\omega_i t \tag{2.9}$$

and according to Fourier-Stieltjes theorem [34],

$$A_i = [2S(\omega)\Delta\omega]^{1/2} \tag{2.10}$$

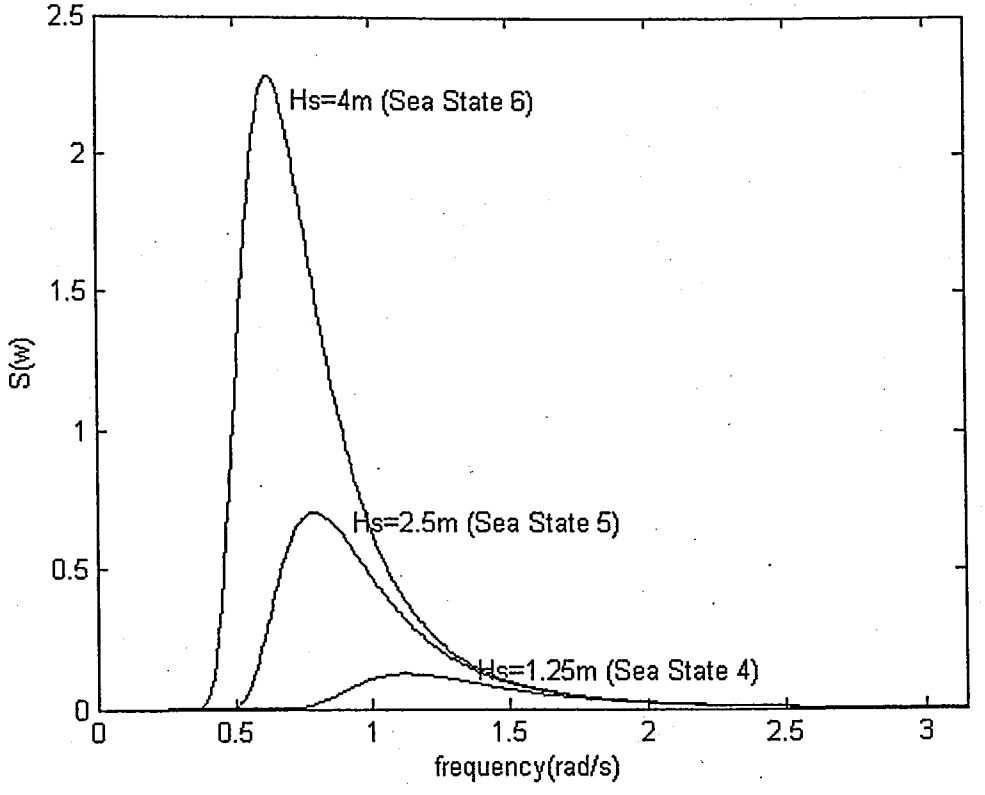

Figure 2.3. Wave spectrums for significant wave heights

Sea waves have two types of effects on ship dynamics as disturbance. One is the disturbance on force dynamics and the other one is the disturbance on moment dynamics [48]. The instantaneous total force in heave can be given in the form,

$$Z_{wave}(t) = Z_1(t) + Z_2(t) \tag{2.11}$$

where

$$\begin{aligned} Z_1(t) &= \sum_{i=1}^{N} Z_{1i}(t), \\ &= \sum_{i=1}^{N} C_{Z1}\nabla\rho(1.5\sin^2\phi + 1)\cdot(1 - 0.02U\cos\phi)F_{1i}\sin\omega_{ei}t, \end{aligned} \tag{2.12}$$

and

$$Z_2(t) = -\sum_{i=1}^{N}\sum_{j=1}^{N}(F_{1i}\sin\omega_{ei}t)\cdot(F_{1j}\sin\omega_{ej}t)\frac{\nabla\rho}{g}\frac{(3+\sin^2\phi)}{10^{|\sin\phi|}} \cdot C_{Z2}(1-0.04U\cos\phi) \tag{2.13}$$

where ω_i is the wave frequency of the i-th component, ∇ is the submarine volumetric displacement, $C_{Z1}, C_{Z2}, C_{M1}, C_{M2}$ are corresponding non-dimensional hydrodynamic coefficients and ϕ is the heading of the submarine relative to the waves. The F_{1i} is the force due to attenuated static head at the vehicle depth produced by wave components,

$$F_{1i} = A_i\omega_i^2\exp(-\frac{\omega_i^2 H_s}{g}) \tag{2.14}$$

where A_i is the wave amplitude of the i-th component.

The instantaneous total moment in pitch can be given in the similar form,

$$M_{wave}(t) = M_1(t) + M_2(t) \tag{2.15}$$

where

$$\begin{aligned} M_1(t) &= \sum_{i=1}^{N} M_{1i}(t), \\ &= \sum_{i=1}^{N} C_{M1}L\nabla\rho(1-0.02U\cos\phi)\,\mathrm{sgn}(\cos\phi)\cdot F_{1i}\cos\omega_{ei}t, \end{aligned} \tag{2.16}$$

and

$$M_2(t) = -C_{M2}L\theta(t)Z_2(t) \tag{2.17}$$

Using the required numeric values given in [2], the force and moment expressions turn out to be,

$$Z_{wave}(t)=\left[2.2772\times10^{5}-1.4552\times10^{4}\sum_{i=1}^{N}F_i\sin\omega_{ei}t\right]\cdot\sum_{i=1}^{N}F_{1i}\sin\omega_{ei}t,$$
$$M_{wave}(t)=1.7780\times10^{7}\cdot\sum_{i=1}^{N}F_i\cos\omega_{ei}t. \tag{2.18}$$

Such a computation of $Z_{wave}(t)$ and $M_{wave}(t)$ is based on sampling $S(\omega)$ at N different frequencies, $\omega_{ei}(i=1,.....,N)$ and obtaining F_i' s (the force due the static head at the vehicle depth) corresponding to these frequencies [2, 34]. Nevertheless, a simple affine form which approximates the expressions in (2.18) is used to model the sea state force and moment effects on submarine for heave and pitch directions [35, 36]:

$$Z_{wave}(t)\approx av(t)+b$$
$$M_{wave}(t)\approx cv(t)+d \tag{2.19}$$

where $v(t)$ is instantaneous sea surface wave elevation, and constants a, b, c, d are determined by data fitting according to (2.18). The numerical values for constants a, b, c, d are given in Table 2.3 for different sea states.

Table 2.3. Constants for sea wave forces and moments [2]

Sea State Code	a	b	c	d
1	-2000	-5	1.65e5	230
2	-15000	-90	1.20e6	8000
3	-28000	-300	2.25e6	3.20e4
4	-48000	-4000	3.90e6	1.65e5
5	-48000	-6700	3.80e6	1.70e5
6	-47000	-11000	3.70e6	2.80e5

2.4. Actuator Dynamics

The submarine model in (2.5) includes three control inputs applied to the system by three actuators. Two of the actuators that are electro-hydraulic systems are used to drive bow and stern hydroplanes. The actuator for the third input is a pump to fill or empty the auxiliary tank. As the actuators are mechanical devices their control action is limited. Limit values for bow and stern hydroplanes are $\pm 30^{\circ}$. A digital filter can represent the dynamics of the bow and stern hydroplanes as [2],

$$\delta B_c(k+1) = 0.885\delta B_c(k) + 0.115\delta B(k) \tag{2.20}$$

and

$$\delta S_c(k+1) = 0.885\delta S_c(k) + 0.115\delta S(k) \tag{2.21}$$

where δB_c and δS_c are the commanded hydroplane deflections, δB and δS are the actual hydroplane deflections.

2.5. Conclusion

General representation of underwater vehicle modeling and coordinate systems are introduced in this part of the dissertation. A classic submarine model is introduced for the depth and pitch angle controls under sea wave effects. Therefore, heave and pitch axis of the submarine model is described in detail.

Modeled submarine is assumed to be at shallow submerged operation at which the sea waves effects the submarines at most. Shallow submerged operation is required when the submarines need to charge the batteries. The submarines are under excessive sea wave effects at shallow submerged operations. Sea waves are modeled by sea wave spectrum approach. The relation between forces and moments acting on the submarine and operation depth is also addressed in this part. Sea wave spectrums with respect to different sea states are also explained in detail. Sea state is a well-known term not only among

world military navy community but also among merchant navy community. Most navy vessels are built in a way to be robust enough to sail up to sea state 6. Therefore, sea states 7, 8 and 9 are not even introduced as it is not realistic to implement a control method on a vessel theoretically not robust to sail at sea states 7, 8 and 9.

Submarine actuators are also modeled and they have saturation and rate limits. These limits are also considered at the submarine model.

3. OBSERVER BASED FAULT DETECTION AND ISOLATION

The term fault is used for any unexpected change of a system function. Fault and failure terms are misinterpreted in some different studies [20, 37]. According to Clark *et al.* (1989), "*a fault is a performance degradation of a system, which even causes some dangerous situation, whereas the later one describes a catastrophic situation of the system performance or even a total breakdown.*"

Fault detection (FD) is a way of making a binary decision in order to find if something is going wrong or not. Fault isolation (FI) is to determine where or which part of the system has a fault. In many practical situations, these two tasks are present together and referred to as Fault Detection and Isolation (FDI).

3.1. Analytical Redundancy

Redundancy is the basic concept, which lies at the heart of most fault detection systems. It can be achieved in two ways; hardware and analytical (software) redundancy. Hardware redundancy is a costly approach for redundancy purposes. As the computer technology is capable to simulate system dynamics, model-based analytical redundancy concept is widely used for redundancy purposes.

Analytical redundancy is a way of detecting faults by comparing actual system response with the analytical model output rather than hardware redundancy. As it is well-known, having redundant systems with extra parallel running hardware is a way of providing redundancy. However, that cannot be achieved for all systems due to space and cost constraints. In order to handle these obstacles, analytical redundancy is used by using model-based FDI approaches. The concept of analytical redundancy uses the information obtained from the model of the system.

Different types of analytical redundancy methods are used for FDI. Among them: observer based approaches [38, 39], which will be described later in detail, the parity space approach [40] and the parameter estimation techniques [41].

The main advantage of analytical redundancy lies in the fact not to use a physical system for redundancy and software is used to provide redundancy. Analytical redundancy methods are surveyed in a study [22] comprehensively.

3.2.Residuals

Residuals are signals that carry information about faults. Comparing actual outputs of the system dynamics with their estimations can generate residuals. The residual signal assumed to be zero when the system is fault free or nominal. It deviates from zero when a fault occurs in system dynamics. Different types of faults can occur in system itself, sensors or actuators. Residuals are insensitive to changes in operating point, disturbances etc., sensitive to faults or changes that have to be detected.

3.2.1. Residual Generation

The residual generation for FDI based on analytical redundancy is represented by a set of differential equations. The faults can occur in system, sensor or actuators as can be seen in Figure 3.1, there are two main ways of generating residuals to detect faults. In many cases, one can either use the estimate of the system output vector y, or the estimate of the system parameter vector θ, namely $\hat{y}$ and $\hat{\theta}$. This leads to the following residual vectors.

$$r_y = y - \hat{y} \qquad \text{and} \qquad r_\theta = \theta - \hat{\theta} \tag{3.1}$$

Generated residual vector is compared with a pre-defined threshold vector in order to detect and isolate the faults. Therefore, residual evaluation is performed as defined in next section.

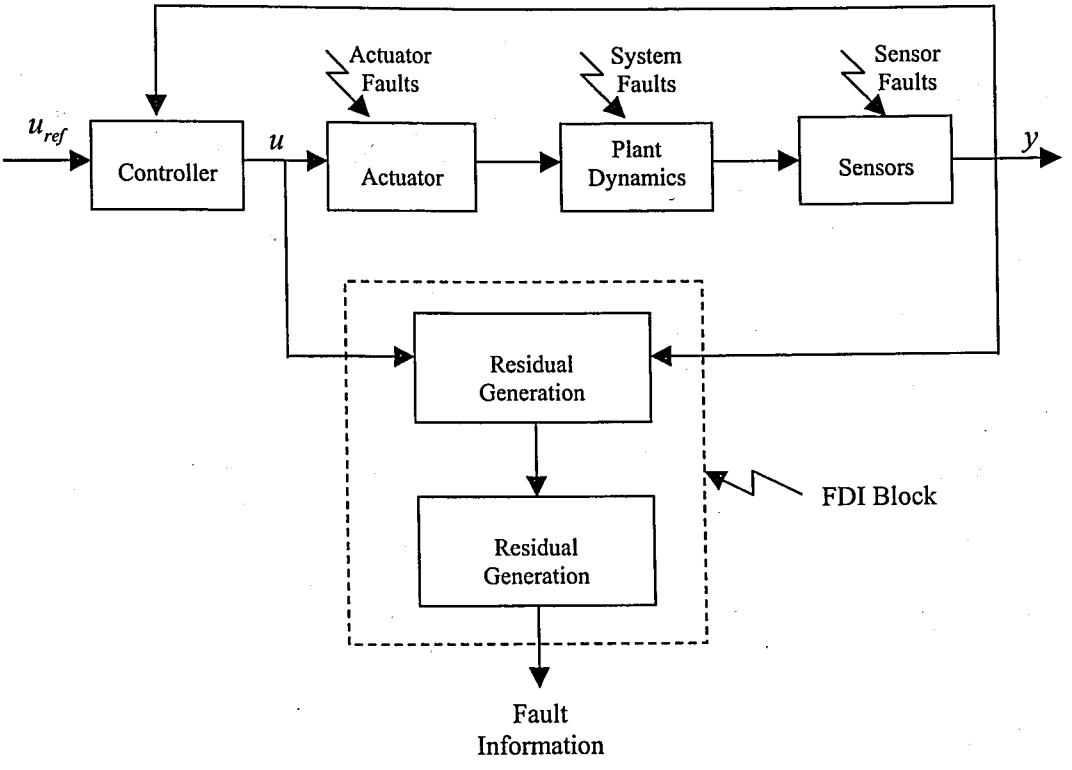

Figure 3.1. General scheme for FDI based on analytical redundancy [20]

3.2.2. Residual Evaluation

FDI requires successful and appropriate residual evaluation. Residual evaluation is the task of evaluating the residuals in order to take the following decisions:

- Is any element of residual vector exceeds the pre-defined threshold vector?
- If yes, which fault(s) is/are present?

Note that the former question is related to fault detection and the latter one for the isolation of the fault.

3.3. Observer-Based FDI Methods

Observer based FDI methods utilize a mathematical model of the plant under fault monitoring. However, in most practical cases, a precise model cannot be obtained. Modeling inaccuracies can be categorized [3] as

- Structured uncertainties,
- Unmodeled or unstructured uncertainties.

Model uncertainty can cause false or missed alarms, hence, it needs to be considered when implementing FDI. There exist several approaches for avoiding false or missed alarms caused by modeling inaccuracies. Obtaining robust residuals by means of observers can solve that drawback.

3.3.1. Luenberger Observer for Fault Detection (FD)

It is stated in many research results on FDI that a reasonable model for FDI purposes is the one which has a description about the system uncertainty, e.g. its distribution matrix or spectral bandwidth. Typical description for the system uncertainty caused by system faults can be represented with a linear state-space model of the system [20], namely,

$$\begin{aligned} \dot{\mathbf{x}}(t) &= \mathbf{A}\mathbf{x}(t) + \mathbf{B}\mathbf{u}(t) + \mathbf{R}\mathbf{f}(t), \\ \mathbf{y}(t) &= \mathbf{C}\mathbf{x}(t). \end{aligned} \tag{3.2}$$

where $\mathbf{x}(t) \in \Re^n$ is the state vector, $\mathbf{u}(t) \in \Re^r$ is the control input vector and $\mathbf{y}(t) \in \Re^m$ is the measurement vector and $\mathbf{f}(t) \in \Re^g$ represents the fault vector which is considered as an unknown time function. Here, $\Re^n$ denotes n-dimensional Euclidean space. On the other hand, **A**, **B** and **C** are system parameter matrices and the pair $\{\mathbf{C}, \mathbf{A}\}$ is assumed to be observable. Here, **R** matrix is the distribution matrix of a system or actuator fault. $\mathbf{Rf}(t)$ term in (3.2) denotes the uncertainty caused by system or actuator faults. For system faults uncertainty is inserted into system matrix **A**, system matrix turns out to be,

$$\mathbf{A}_{fault} = \mathbf{A} + \Delta\mathbf{A} \tag{3.3}$$

Uncertainty is inserted into control input matrix **B** for actuator faults, and

$$\mathbf{B}_{fault} = \mathbf{B} + \Delta\mathbf{B} \tag{3.4}$$

Hence, $\mathbf{Rf}(t)$ in (3.2) can be represented with respect to fault as follows,

$$\mathbf{Rf}(t) = \begin{cases} \Delta\mathbf{A}\mathbf{x}(t) & \text{system fault} \\ \Delta\mathbf{B}\mathbf{x}(t) & \text{actuator fault} \end{cases} \tag{3.5}$$

By means of an observer, the residual can be generated as,

$$\dot{\hat{\mathbf{x}}}(t) = (\mathbf{A} - \mathbf{LC})\hat{\mathbf{x}}(t) + \mathbf{B}\mathbf{u}(t) + \mathbf{L}\mathbf{y}(t), \tag{3.6}$$

and

$$\begin{aligned} \hat{\mathbf{y}}(t) &= \mathbf{C}\hat{\mathbf{x}}(t), \\ \mathbf{r}(t) &= \mathbf{y}(t) - \hat{\mathbf{y}}(t) = \mathbf{C}\left[\mathbf{x}(t) - \hat{\mathbf{x}}(t)\right]. \end{aligned} \tag{3.7}$$

where $\mathbf{r}(t) \in \Re^p$ is the residual vector, $\hat{\mathbf{x}}$ and $\hat{\mathbf{y}}$ are state and output estimates. By defining the state estimation error as

$$\mathbf{e}(t) = \mathbf{x}(t) - \hat{\mathbf{x}}(t) \tag{3.8}$$

error dynamics can be written as,

$$\dot{\mathbf{e}}(t) = (\mathbf{A} - \mathbf{LC})\mathbf{e}(t) + \mathbf{Rf}(t), \tag{3.9}$$

Also note that,

$$\mathbf{r}(t) = \mathbf{C}\mathbf{e}(t). \tag{3.10}$$

3.3.2. Dedicated Observer Scheme for FDI

The dedicated observer scheme (DOS) for FDI purposes was first introduced in [14]. The scheme was based on the idea that a separate state observer for each sensor to be monitored was designed and used for FDI purposes.

This scheme was one of the first FDI methods based on the analytical redundancy. If there are m sensors there must be m separate observers designed for that scheme to detect the possible system or actuator faults, which might occur. Figure 3.2 depicts the basic internal structure of the FDI system using DOS. System dynamics are monitored by means of observers dedicated to each state of the system. The thresholds are defined with respect to known possible faults for fault detection logic. If one of the observed states of the system dynamics exceeds the pre-defined threshold value then, that system component is warned as faulty part to operator.

Consider the dynamic system in (3.2), the fault in the i^{th} system output can be detected as shown in Figure 3.2 by dedicating one observer for each system output. A fault in system dynamics appears to effect system matrix **A** as defined in (3.3) and a fault in the actuator appears to effect actuator as defined in (3.4).

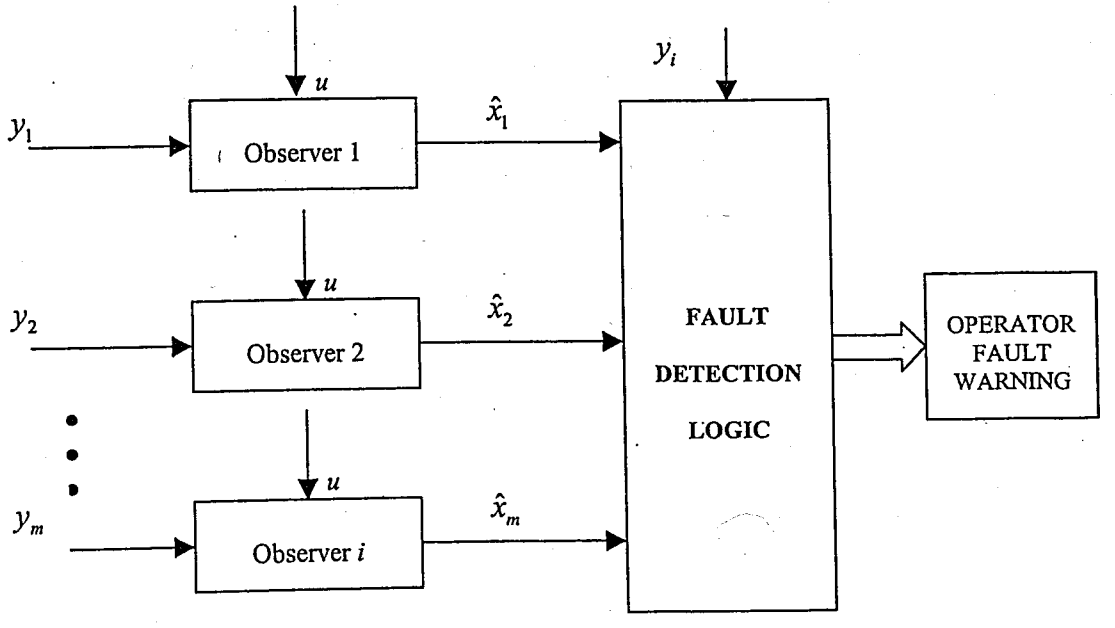

Figure 3.2. The dedicated observer scheme [28]

There are m states of the system in (3.1) and it is assumed that none of these m instruments are redundant. m observers are designed and m threshold values are defined for each fault which might occur at each state of the system dynamics.

For residual generation, the states are observed with a full-order Luenberger observer as defined in (3.6) and from the observed states and actual system states, the residual vector can be generated as;

$$\mathbf{r}(t) = \mathbf{x}(t) - \hat{\mathbf{x}}(t) \tag{3.11}$$

where $\mathbf{x} = [x_1 \ldots\ldots x_i]$ and $\hat{\mathbf{x}} = [\hat{x}_1 \ldots\ldots \hat{x}_i]$.

3.3.3. Linear Unknown Input Observer for FDI

It is aimed to design an observer in order to detect and isolate the faults of a dynamic system by de-coupling fault effects from system dynamics and generating a residual which is robust to the vector of unknown inputs of system dynamics.

The robust observer schemes for FDI has been used by means of different types of observer design approaches, one of which is known as unknown input observer (UIO) and has been proposed by [42]. The observer design with unknown input approach has been described in detail in [20]. Consider the dynamic system model with system uncertainty as an additive term slightly different to system representation defined in (3.2),

$$\begin{aligned} \dot{\mathbf{x}}(t) &= \mathbf{A}\mathbf{x}(t) + \mathbf{B}\mathbf{u}(t) + \mathbf{E}\mathbf{d}(t), \\ \mathbf{y}(t) &= \mathbf{C}\mathbf{x}(t). \end{aligned} \tag{3.12}$$

where $\mathbf{d}(t)$ is the unknown input vector which represents the dynamics of the system uncertainties or disturbances. In order to overcome the false alarm of faults due to system uncertainty $\mathbf{d}(t)$ in (3.12), observer should be designed in a way to be robust with respect to unknown inputs. As it is mentioned before, the faults in system dynamics can occur in actuators, system itself and sensors. Here, it is assumed that the distribution matrix $\mathbf{E}$ is

known. By using the information obtained from **E**, the unknown input $\mathbf{d}(t)$ can be de-coupled from the residual information.

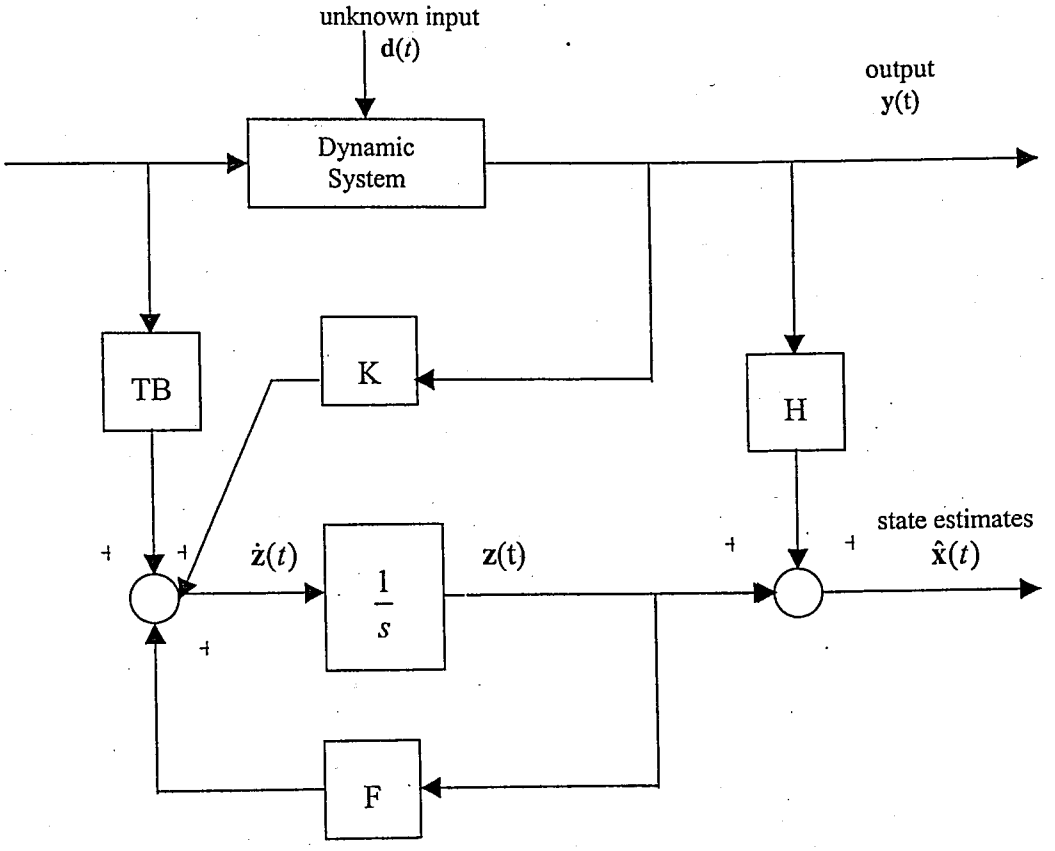

Figure 3.3. The Structure of linear UIO [20]

The structure for a full-order UIO is given as,

$$\begin{aligned} \dot{\mathbf{z}}(t) &= \mathbf{F}\mathbf{z}(t) + \mathbf{T}\mathbf{B}\mathbf{u}(t) + \mathbf{K}\mathbf{y}(t), \\ \hat{\mathbf{x}}(t) &= \mathbf{z}(t) + \mathbf{H}\mathbf{y}(t). \end{aligned} \tag{3.13}$$

where $\hat{\mathbf{x}}(t)$ is the estimated state vector and z is the state of observer. **F**, **T**, **K** and **H** are matrices designed in order to de-couple the effects of $\mathbf{d}(t)$ from (3.12), as

$$\begin{aligned} &(\mathbf{HC} - \mathbf{I})\mathbf{E} = \mathbf{0}, \\ &\mathbf{T} = \mathbf{I} - \mathbf{HC}, \\ &\mathbf{F} = \mathbf{A} - \mathbf{HCA} - \mathbf{K}_1\mathbf{C}, \\ &\mathbf{K}_2 = \mathbf{FH}. \end{aligned} \tag{3.14}$$

with **0** and **I** denoting zero and identity matrices, respectively, of appropriate dimensions. The state estimation error under these conditions can be computed from Figure 3.3 as using (3.8), (3.12)-(3.14),

$$\begin{aligned}\dot{\mathbf{e}}(t) &= (\mathbf{A}-\mathbf{HCA}-\mathbf{K}_1\mathbf{C})\mathbf{e}(t)+[\mathbf{F}-(\mathbf{A}-\mathbf{HCA}-\mathbf{K}_1\mathbf{C})]\mathbf{z}(t)\\ &\quad+[\mathbf{K}_2-(\mathbf{A}-\mathbf{HCA}-\mathbf{K}_1\mathbf{C})\mathbf{H}]\mathbf{y}(t)\\ &\quad+[\mathbf{T}-(\mathbf{I}-\mathbf{HC})]\mathbf{B}\mathbf{u}(t)+(\mathbf{HC}-\mathbf{I})\mathbf{E}\mathbf{d}(t)\end{aligned} \tag{3.15}$$

where

$$\mathbf{K}=\mathbf{K}_1+\mathbf{K}_2 \tag{3.16}$$

when the conditions in (3.14) are held,

$$\dot{\mathbf{e}}(t)=\mathbf{F}\mathbf{e}(t), \tag{3.17}$$

If all eigenvalues of **F** are stable, the derivative of estimation error $\dot{\mathbf{e}}(t)$ will approach zero asymptotically.

The design algorithm can be expressed in a compact form as follows;

(i) If $rank(\mathbf{CE}) \neq rank(\mathbf{E})$, then an UIO design does not exist go to (v), otherwise,

(ii) Compute **H**, **T** and $\mathbf{A}_1$ matrices as,

$$\mathbf{H}=\mathbf{E}[(\mathbf{CE})^T\mathbf{CE}]^{-1}(\mathbf{CE})^T,\quad \mathbf{T}=\mathbf{I}-\mathbf{HC},\quad \mathbf{A}_1=\mathbf{TA},$$

(iii) Check the observability of the plant: If (**C**, **A**) is observable then an UIO exists, otherwise an observable canonical form should be applied to (**C**, $\mathbf{A}_1$),

(iv) Compute **F** and **K** to hold the conditions in (3.15) and the derivative of the estimation error $\dot{\mathbf{e}}(t)$;

$$\mathbf{F}=\mathbf{A}_1-\mathbf{K}_1\mathbf{C},\quad \mathbf{K}=\mathbf{K}_1+\mathbf{K}_2=\mathbf{K}_1+\mathbf{FH},$$

(v) STOP.

In order to detect a particular fault caused by an actuator or sensor, the residual has to be robust to unknown inputs but sensitive to mentioned faults. The system representation in (3.12) can be modified to express the sensor and actuator faults in the system model as [20],

$$\begin{aligned} \dot{\mathbf{e}}(t) &= (\mathbf{A}_1 - \mathbf{K}_1\mathbf{C})\mathbf{e}(t) + \mathbf{TB}\mathbf{f}_a(t) - \mathbf{K}_1\mathbf{f}_s(t) - \mathbf{H}\mathbf{f}_s(t), \\ \mathbf{r}(t) &= \mathbf{C}\mathbf{e}(t) + \mathbf{f}_s(t). \end{aligned} \tag{3.18}$$

It can easily be seen that unknown input vector $\mathbf{d}(t)$ effects de-coupled from the derivative of state estimation error and residual vectors. The residual vector in (3.18) can be used in a way to detect the faults by means of the threshold logic as described in Section 3.3.3. But this holds true if $\mathbf{TB} \neq 0$, otherwise, actuator fault vector vanishes from the derivative the state estimation error equation.

$$\begin{aligned} \|\mathbf{r}(t)\| &< \varphi \text{ for nominal case,} \\ \|\mathbf{r}(t)\| &\geq \varphi \text{ for faulty case,} \end{aligned} \tag{3.19}$$

where φ stands for threshold vector and vector norm definition is given in Appendix B.

3.4. Examples

In this section some examples are given in order to justify the methods explained in previous sections.

3.4.1. Case Study: Fault Detection on a Pneumatic Valve

3.4.1.1. System Model. A pneumatic servo system linear model is used for SISO-system FD case study. The servo system consists of 6 main parts; the spool valve and its controller, the cylinder, the load, the system controller and the position feedback

potentiometer [43]. The transfer function for the system can be obtained by combining the governing equations for each system component.

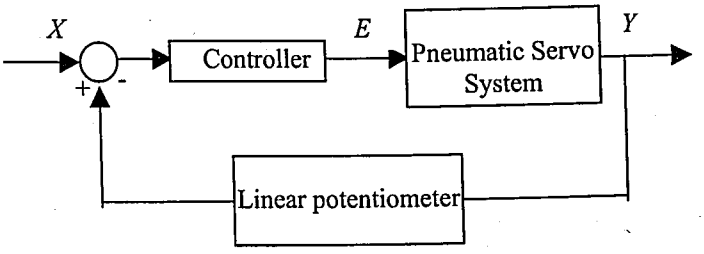

Figure 3.4. Pneumatic servomechanism block diagram [44]

The mathematical equations for each part is derived from the dynamic, energy and flow equations. The equations of a pneumatic servo mechanism form a complicated set of coupled nonlinear differential equations. These nonlinear equations are too complicated for design purposes. A detailed derivation of these equations is given by [44]. Therefore, they need to be linearised and simplified, under the following assumptions:

- Valve spool position is proportional to the input voltage about a desired operating point. Hence, the third order dynamics of valve can be neglected.
- For cylinder ram dynamics, perfect-gas, fast-process, good-insulation, horizontal-orientation assumptions are made.
- For linearisation, it is assumed that changes about a steady-state initial condition is very small and the piston is initially at the central position.

Using all these assumptions, the equations of a pneumatic servo mechanism can be linearised around an equilibrium point. The continuous-time transfer function describing this linearised dynamics of the servo system is then obtained as [45]

$$H(s)=\frac{Y(s)}{E(s)}=\frac{1100}{s^3+181s^2+561s} \tag{3.20}$$

where the output $Y(s)$ is the position of the cylinder and the input $E(s)$ is the valve solenoid voltage.

An internal feedback loop within the servo system is introduced [45].

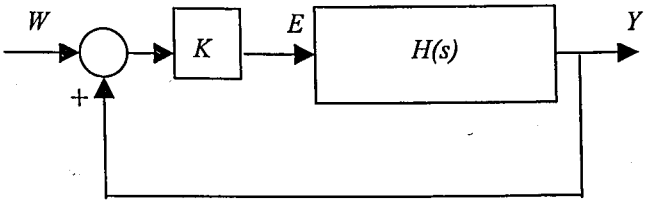

Figure 3.5. Block diagram of the internal loop [44]

The proportional gain K in Figure 3.5 is tuned in such a way that the system is forced to behave like a 2nd order over-damped system. To avoid the effect of this in tracking performance, the largest possible value of K is used, which do not cause overshooting. It is calculated to be K=0.7 and with this gain value the closed loop transfer function is obtained as

$$G_c(s)=\frac{Y(s)}{W(s)}=\frac{770}{s^3+181s^2+561s+770} \tag{3.21}$$

where $W(s)$ is the input voltage to the inner loop. Closing the loop, a pole is positioned away from the imaginary axis, which can be neglected with respect to the other two poles. Hence, it is obtained,

$$G_c(s)\approx\frac{770}{s^2+3.13s+4.33}, \tag{3.22}$$

Further, a feedforward attenuation is required to impose a unity gain, i.e.,

$$G_c(s)\approx\frac{4.33}{s^2+3.13s+4.33}. \tag{3.23}$$

3.4.1.2. Fault Detection Using Luenberger Observer. The residual from a Luenberger observer is used to detect the fault in the system. The transformation of the servo system model from transfer function representation in (3.23) to state-space representation [43] yields the model

$$\begin{bmatrix}\dot{x}_1\\ \dot{x}_2\end{bmatrix}=\begin{bmatrix}0 & 1\\ -4.33 & -3.13\end{bmatrix}\begin{bmatrix}x_1\\ x_2\end{bmatrix}+\begin{bmatrix}0\\ -4.33\end{bmatrix}u(t),$$
$$y(t)=\begin{bmatrix}0 & 1\end{bmatrix}x(t). \tag{3.24}$$

Here, the system is a SISO system, the observability of the system in (3.24) is checked as,

$$rank([\mathbf{C} \quad \mathbf{CA}])=2, \tag{3.25}$$

The dynamic system is completely observable. The observer dynamics is required to be much faster than the system dynamics. The eigenvalues of the full-state observer defined to be;

$$\lambda_1=14 \qquad \lambda_2=100 \tag{3.26}$$

The observer gain vector $\mathbf{K}_e$ can be obtained by means of pole-placement method defined in [46],

$$\mathbf{K}_e=\begin{bmatrix}17.13\\ 50.7131\end{bmatrix} \tag{3.27}$$

The residual can be generated from (3.10) and a pre-defined threshold can be used to detect the fault as defined in (3.19).

3.4.1.3 Simulation Results. FD scheme with Luenberger observer is simulated with MATLAB-SIMULINK software. Here a bias fault of 10 per cent is created at the 2nd second of the simulation and a residual generated as defined in (3.10) which can be seen in Figure 3.6. In other words the system parameters are changed to 10 per cent greater values in order to insert a system fault.

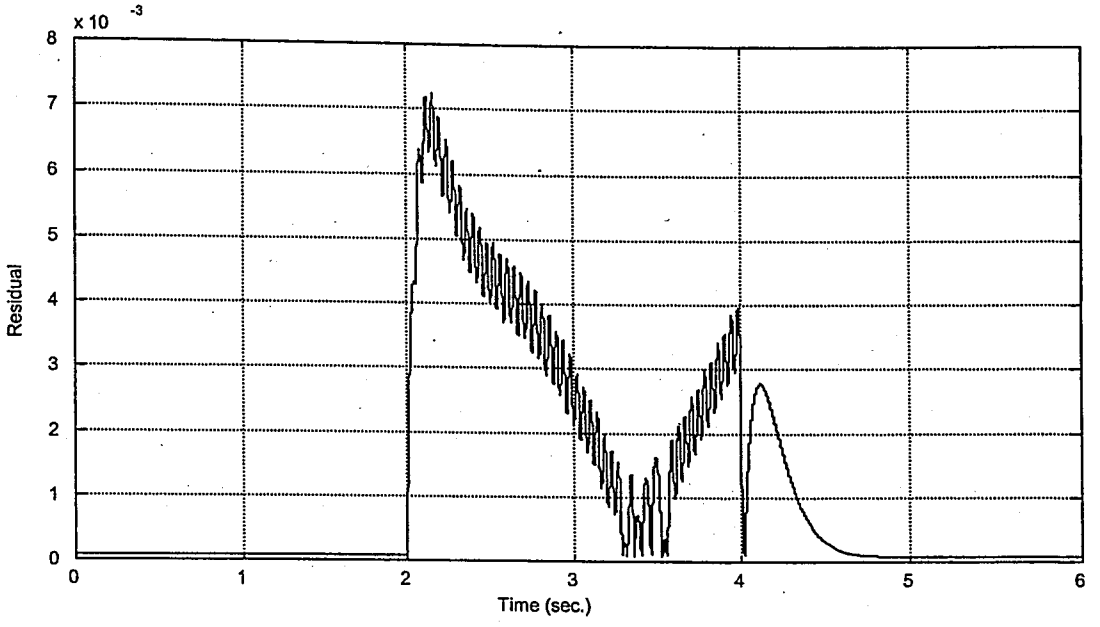

Figure 3.6. Residual generated with estimated and actual outputs of the system [43]

FD scheme detected the fault when the residual value exceeded the pre-defined threshold value. At the 4th second of the simulation, the pneumatic servo mechanism is initiated to act nominally which can be seen from Figure 3.6.

3.4.2. Case Study: MIMO System FDI

In this case, it is assumed that there is no disturbance for modelling uncertainty or at least modelling uncertainty can be handled with sliding-mode controller. On the other hand, a typical description for the system uncertainty caused by system faults can be represented with the following linear model of the system as given in (3.2) [47, 48].

Consider state-space representation of a Multi-Input-Multi-Output (MIMO) system as [47, 48],

$$\begin{aligned} \dot{\mathbf{x}}(t) &= \begin{bmatrix} -2 & 0.1 \\ 2 & 3 \end{bmatrix} \mathbf{x}(t) + \begin{bmatrix} 5 & 0 \\ 0 & 1 \end{bmatrix} \mathbf{u}(t), \\ \mathbf{y}(t) &= \begin{bmatrix} 1 & 0 \\ 0 & 1 \end{bmatrix} \mathbf{x}(t) \end{aligned} \tag{3.28}$$

A system fault is inserted into the system matrix **A**, consequently, the state space representation of the faulty system becomes,

$$\begin{aligned}\dot{\mathbf{x}}(t) &= \begin{bmatrix} 6 & 10 \\ 20 & 5 \end{bmatrix}\mathbf{x}(t) + \begin{bmatrix} 5 & 0 \\ 0 & 1 \end{bmatrix}\mathbf{u}(t), \\ \mathbf{y}(t) &= \begin{bmatrix} 1 & 0 \\ 0 & 1 \end{bmatrix}\mathbf{x}(t)\end{aligned} \tag{3.29}$$

The MIMO linear system given as an example has two eigenvalues, one of them being negative and the other is positive, namely,

$$\mu_1 = -2.0397 \qquad \mu_2 = 3.0397 \tag{3.30}$$

The fault inserted into system matrix **A** and the eigenvalues of the system turns out to be,

$$\alpha_1 = 19.6510 \qquad \alpha_2 = -8.6510 \tag{3.31}$$

It can easily be checked that the state vector is observable from both outputs.

A linear observer is designed to observe the system outputs with the following gain matrix which in return provides a faster response for observers for each output.

$$\mathbf{L} = \begin{bmatrix} 21 & 32.1 \\ 1692 & 21 \end{bmatrix} \tag{3.32}$$

The fault can be detected by means of the residual vector by means of threshold vector similar to the approach defined in (3.19). The above mentioned fault has been inserted into system matrix **A** at 1.25^{th} sec. and removed at 1.75^{th} sec. of the simulation. MATLAB-SIMULINK software has been used for simulations.

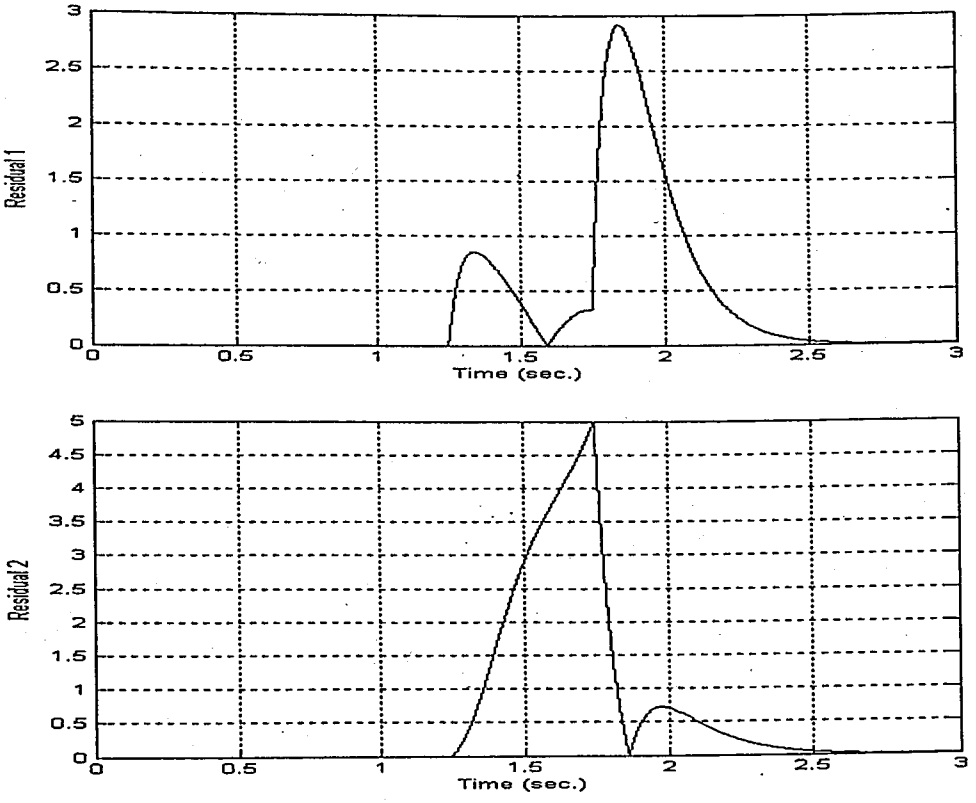

Figure 3.7. Components of residual vector [47]

Fault can be detected by means of residual vector **r** as the residual vector components can be seen in Figure 3.7. Mentioned residuals can be used in order to detect the faults and extract fault distribution information.

4. RECONFIGURING SLIDING-MODE CONTROLLER

The reconfiguring control for fault accommodation purposes has usually been achieved by mainly adaptive controllers [11, 19]. To my knowledge, the novel idea proposed is the first application of a sliding-mode control scheme as an active reconfiguring controller for fault accommodation.

The fault distribution matrix extracted by means of a linear observer is used in two approaches: First one is to adaptively switch the corrective gain vector of the sliding-mode controller. Here, the fault distribution information is used as the corrective gain vector to compensate the uncertainty inserted into the system dynamics due to system fault. The second one is to adjust the equivalent control term of sliding mode controller, while having a small gain value for the corrective gain part.

Applicability of the proposed algorithm with both approaches is shown in the reconfiguration of a sliding-mode controller for a MIMO linear system. The objective of the controller is to control the MIMO system under nominal operating condition, as well as in case of an abrupt fault. The mentioned reconfigured controller is switched back to its nominal scheme when fault detection scheme detects that the faulty system component acts nominally.

The proposed method aims to avoid chattering for the nominal plant, nevertheless, to keep the process in operation by increasing the robustness of the controller with a larger gain for the faulty plant in accordance with the size of the fault distribution matrix. It is required to avoid an increase in the controller gain and, hence, in the chattering, for the nominal plant; but for the faulty plant the robustness is a delicate subject to be considered to keep the plant running with an acceptable performance. Here, a trade-off appears between the tracking performance and chattering [3].

The proposed algorithm can be implemented for autonomous underwater and space vehicles when there is no way to stop the process and fix the faulty system component. Torpedo and missile guidance systems can also be considered as military applications.

4.1. Sliding-Mode Controllers

Consider the SISO system defined below,

$$\dot{x} = f(x) + b(x)u, \tag{4.1}$$

where x is the state variable,

$f(x)$ is the unknown dynamics,
u is the control input and
$b(x)$ is the input gain

Given the initial conditions, perfect tracking $x \equiv x_d$ is equivalent to keeping the states on the sliding surface $s(t)$ for all $t > 0$. This condition, i.e., $s \equiv 0$ represents a linear differential equation with unique solution of $\tilde{x} \equiv 0$. Considering the dynamic system in (4.1), a switching surface is defined as [3],

$$s(x) = \tilde{x} + \lambda \int \tilde{x}\, dt \tag{4.2}$$

where s is the scalar function, λ is a positive scalar, which defines the slope of the surface and $\tilde{x}$ is the tracking error which is the difference between actual and desired trajectories and defined as,

$$\tilde{x} = x - x_d \tag{4.3}$$

In order to make the system follow the desired trajectory, a Lyapunov function is defined in form of s,

$$V = \frac{1}{2}s^2 \tag{4.4}$$

which is positive definite. It is required that the following condition must be satisfied for overall system to be stable under the switching controller inputs,

$$\dot{V} < 0 \qquad \forall t > 0 \tag{4.5}$$

Control law u outside of sliding surface is chosen in a way to keep the scalar s at zero can be achieved under the condition [3],

$$\frac{1}{2}\frac{d}{dt}s^2 \leq -\eta|s| \tag{4.6}$$

where η is a strictly positive constant. In fact, (4.6) defines the squared distance to the surface. The system trajectories stay on the surface once on the surface.

From (4.2), first derivative of sliding surface function becomes,

$$\dot{s}(t) = \dot{\tilde{x}}(t) + \lambda\tilde{x}(t) = 0, \tag{4.7}$$

It follows from (4.1), (4.2) and (4.7) that,

$$\dot{s}(t) = fx(t) + bu(t) - \dot{x}_d - \lambda\tilde{x}(t) \tag{4.8}$$

Assume that the dynamics of f has some uncertainties and estimated with a boundary as follows

$$\left|f - \hat{f}\right| \leq F \tag{4.9}$$

and the best approximation of a control law $\hat{u}$ in order to keep the system states on the sliding surface and achieve $\dot{s} = 0$ is obtained as,

$$\hat{u} = \frac{1}{b}[-\hat{f} + \dot{x}_d - \lambda\dot{\tilde{x}}] \tag{4.10}$$

In order to satisfy the condition in (4.6), despite uncertainties in f, a discontinuous term is added on to $\hat{u}$ and, hence, the overall controller with the corrective control term will be given as,

$$u = \frac{1}{\hat{b}}[\hat{u} - k\,\mathrm{sgn}(s)] \tag{4.11}$$

where

$$\mathrm{sgn}(s) = \begin{cases} +1, & if\ s > 0 \\ 0, & if\ s = 0 \\ -1, & if\ s < 0 \end{cases} \tag{4.12}$$

Inserting (4.11) into (4.8), one will obtain,

$$\dot{s} = (f - \frac{b}{\hat{b}}\hat{f}) + (1 - \frac{b}{\hat{b}})(-\dot{x}_d + \lambda\tilde{x}) - \frac{b}{\hat{b}}k\,\mathrm{sgn}(s) \tag{4.13}$$

so that k must hold the following condition,

$$k \geq \left|\frac{\hat{b}}{b}f - \hat{f} + (\frac{\hat{b}}{b} - 1)(-\dot{x}_d + \lambda\tilde{x})\right| + \eta\frac{\hat{b}}{b} \tag{4.14}$$

f term can be expressed in terms of $\hat{f}$ as

$$f = \hat{f} + (f - \hat{f}) \tag{4.15}$$

Hence,

$$k \geq \hat{b}b^{-1}F + \eta\hat{b}b^{-1} + \left|\hat{b}b^{-1} - 1\right| \cdot \left|\hat{f} - \dot{x}_d + \lambda\tilde{x}\right| \tag{4.16}$$

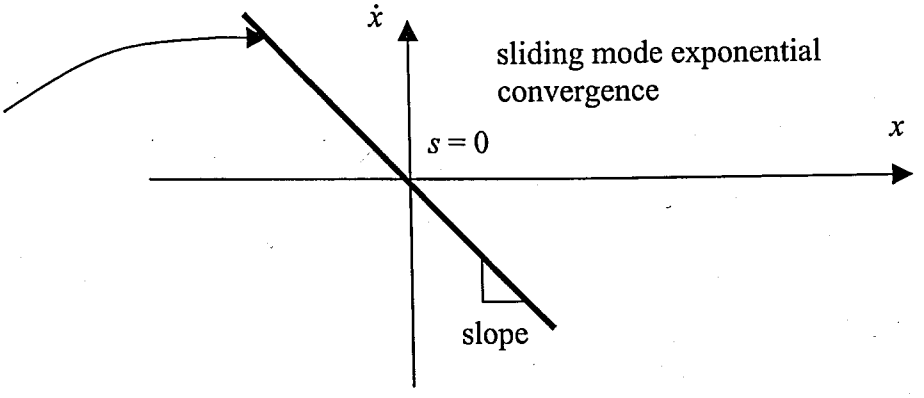

Figure 4.1. Graphical illustration of sliding surface [3]

Once the state errors are on the sliding surface, they will converge to the origin in the dynamics defined by the sliding surface. In order to compensate the effects of drifting away from the sliding surface and guarantee a sliding regime on the sliding surface shown in Figure 4.1, a nonlinear switching function is used as corrective gain.

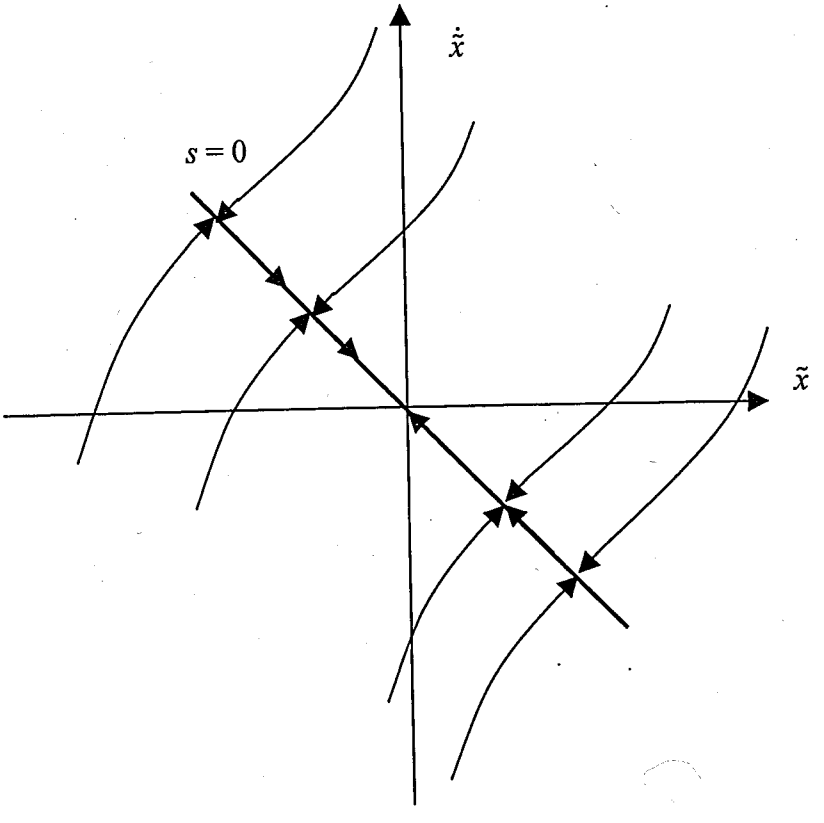

Figure 4.2. A typical phase portrait under sliding-mode control [26]

4.1.1. Chattering Phenomenon

The main drawback of sliding mode control is chattering due to delays and imperfections [3, 49, 50] as depicted in Figure 4.3.

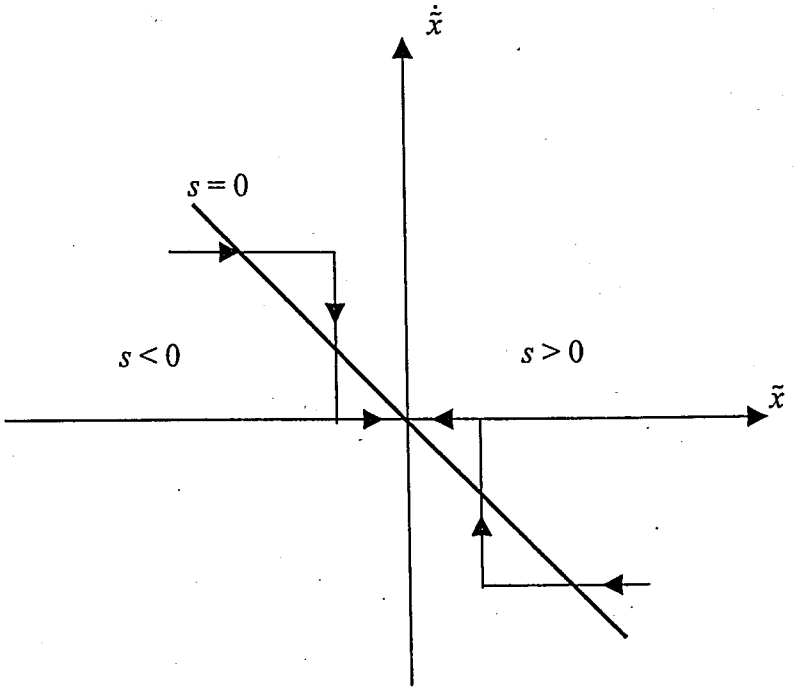

Figure 4.3. Chattering phenomenon of sliding mode controller [26]

The so-called chattering drawback of sliding mode controllers can be eliminated to some degree by means of soft nonlinear functions. In this case, instead of a hard nonlinearity as signum function defined in (4.12), a soft nonlinear function such as saturation function

$$sat(\frac{\mathbf{s}}{\Phi}) = \begin{cases} +1 \ if \ \ \mathbf{s} > \Phi \\ \mathbf{s} \ \ if \ \ -\Phi \le \mathbf{s} \le \Phi \\ -1 \ if \ \ \mathbf{s} < \Phi \end{cases} \tag{4.17}$$

can be used in order to eliminate chattering.

If Equations (4.12) and (4.17) are compared, it is seen that there is an extra Φ term which defines a layer around rather than on the sliding surface and relaxes the switching line.

This relaxation eliminates the chattering but in return, the tracking performance of the sliding mode controller will decrease. There is a trade-off between eliminating chattering and tracking performance. The boundary layer described above can be seen in Figure 4.4 [3].

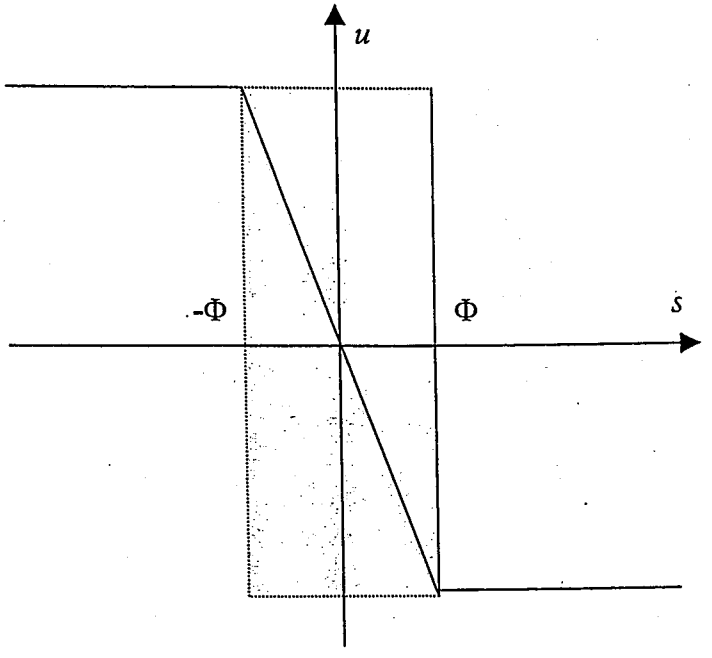

Figure 4.4. The boundary layer and control input [3]

4.2. Reconfiguring Controller Idea

The basic idea is to design a controller using sliding-mode methodology, which can yield satisfactory performance when uncertainties inserted into the process at any instant. The robustness against a fault should be adjusted in such a way that the proposed sliding-mode controller should increase the corrective gain when a fault is detected and decrease the gain when the system acts nominally. Hence, the novel idea of this study is a synergic combination of sliding-mode control method and fault detection methods.

The relation between robustness and the size of the controller gain has been illustrated below with examples. Here the corrective gain forces the response to the defined sliding surface and equivalent control part tries to keep the response on the sliding surface, in return the stability is achieved asymptotically. It is observed that nominal plants require

less corrective gain and causes less chattering. Even any classical control technique such as PID controller could have been used for this part. Nevertheless, it would have failed if a fault develops in the system.

4.2.1. Increased Corrective Gain for Faulty Case

By combining fault detection techniques defined in Section 3.4. with the standard sliding-mode control approach, it is possible to introduce a high switching gain only when necessary. This idea implemented on the linear model of pneumatic servomechanism mentioned in Chapter 3 and where transfer function is given in (3.23).

The controller is designed so as to be robust against the model uncertainties and self-reconfiguring with switched higher corrective gain if a fault occurs in the system. The corrective gain, which is switched to in case of a fault is obtained with prior information of the fault.

The control of the pneumatic servomechanism is achieved by controlling the servo control valve. It is a tracking problem and a desired trajectory has to be followed by the piston of the servomechanism.

4.2.1.1. SISO Switched-Gain Sliding-Mode Controller. The differential equation corresponding to (3.23) can be written as,

$$\ddot{x}(t) = -3.13\dot{x}(t) - 4.33x(t) + 4.33u(t), \tag{4.18}$$

By inserting (4.18) into (4.7),

$$\dot{s}(t) = -3.13\dot{x}(t) - 4.33x(t) + 4.33u(t) - \ddot{x}_d(t) + \lambda\dot{\tilde{x}}(t), \tag{4.19}$$

and, from (4.8), it follows that

$$u_{eq}(t) = \frac{1}{4.33}(3.13\dot{x}(t) + 4.33x(t) + \ddot{x}_d(t) - \lambda\dot{\tilde{x}}(t)). \tag{4.20}$$

This is the equivalent control for the given system, a corrective control term is added to this equivalent control term, which has discontinuous characteristics. Then, the control turns out to be,

$$u(t) = \frac{1}{4.33}(3.13\dot{x}(t) + 4.33x(t) + \ddot{x}_d(t) - \lambda\dot{\tilde{x}}(t)) - k\,\mathrm{sgn}(s). \tag{4.21}$$

The nominal gain k for corrective gain of sliding mode controller can be defined in (4.16). By choosing k large enough, the sliding condition is guaranteed.

For the nominal case the controller turns out to be,

$$u(t) = \frac{1}{4.33}(3.13\dot{x}(t) + 4.33x(t) + \ddot{x}_d(t) - \lambda\dot{\tilde{x}}(t)) - k_{nom}\,\mathrm{sgn}(s) \tag{4.22}$$

Under the faulty condition the controller would be given as,

$$u(t) = \frac{1}{4.33}(3.13\dot{x}(t) + 4.33x(t) + \ddot{x}_d(t) - \lambda\dot{\tilde{x}}(t)) - k_{fault}\,\mathrm{sgn}(s). \tag{4.23}$$

4.2.1.2. Simulation Results. The proposed controller is simulated with Matlab-Simulink Software. The nominal gain term k_{nom} is implemented as 6 for the nominal plant and the faulty case gain term k_{fault} is implemented as 20 for the faulty plant. The fault is simulated by abruptly changing the parameters of the closed-loop system. The residual is obtained from (3.10). The residual exceeds a pre-defined threshold, then, the fault is detected and the sliding-mode controller is switched corrective gain to obtain the desired response for the faulty plant.

The results for nominal and faulty plant cases can be seen together in Figures 4.5-4.8. Here a bias fault [43] of 10% created at the 2nd sample and fault detection system

shown in Figure 4.5 and switched the sliding-mode controller gain. At the 4th second, the servomechanism is simulated to act nominally and it is observed that the sliding mode controller gain switched back to the corrective gain which is calculated for the nominal case. The controller switched to a higher pre-defined gain value after fault is detected by the FD mechanism. Satisfactory tracking is achieved as can be seen from trajectory error in Figure 4.8.

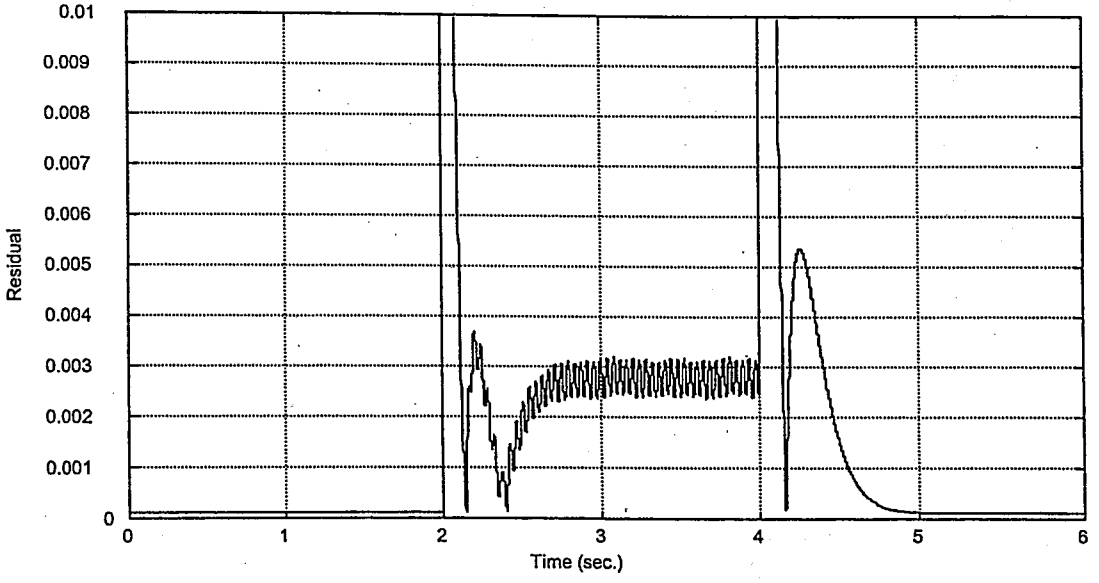

Figure 4.5. Residual for pneumatic servomechanism

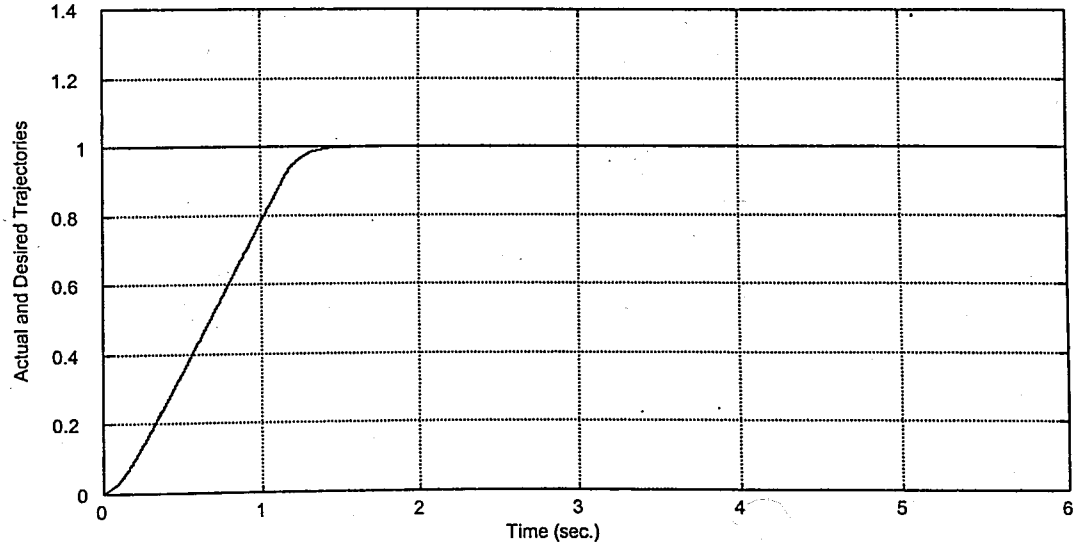

Figure 4.6. Actual and desired trajectories

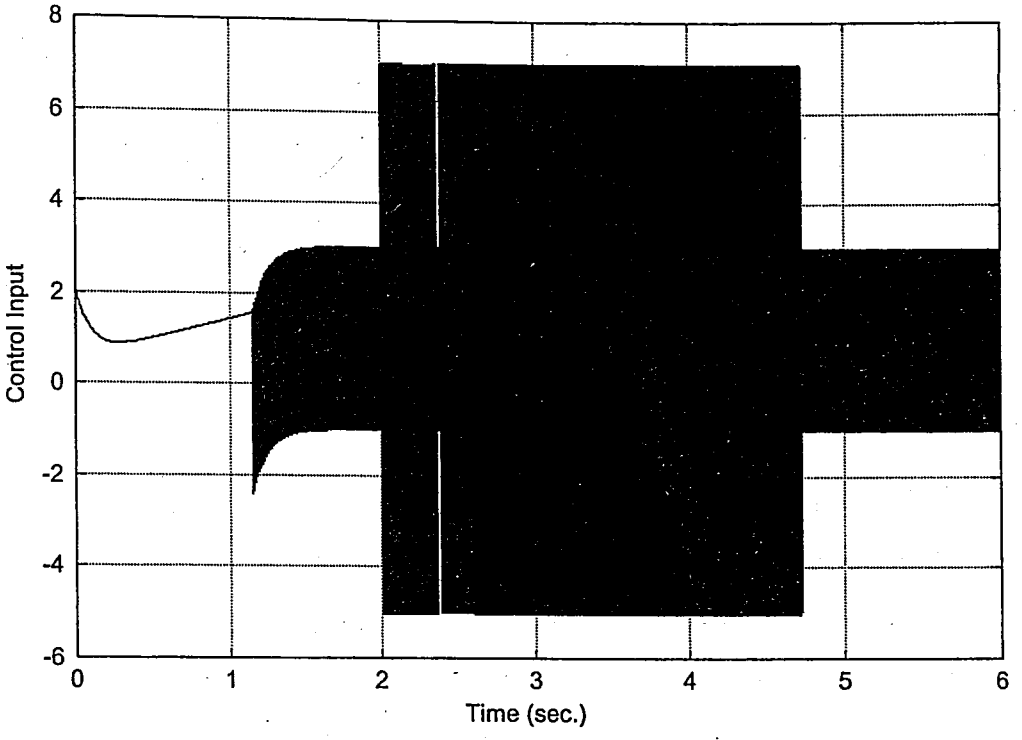

Figure 4.7. Switching controller for nominal and faulty plant

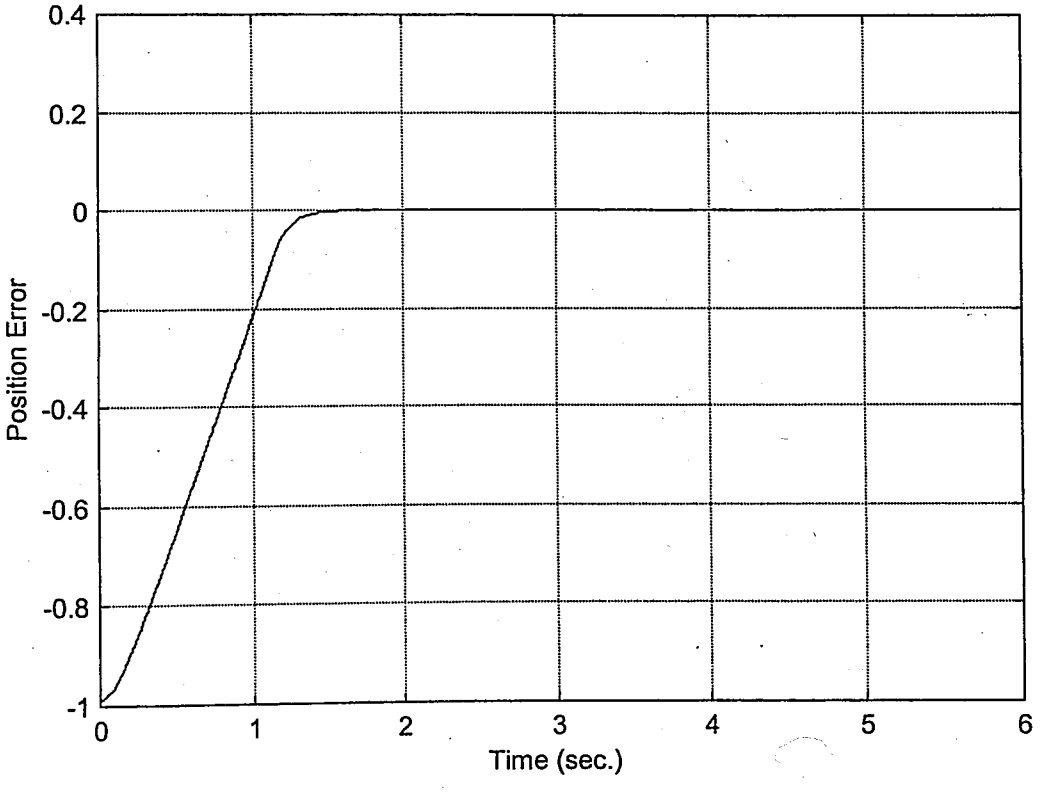

Figure 4.8. Trajectory error

4.3. Fault Distribution Information

It is required to reconfigure the sliding mode controller structure and adjust the controller gain according to the fault information, without referring to any prior information about the faults which might occur in the system. Therefore, the next step is to find an analytical relation between robustness of the sliding-mode controller and fault information. Therefore, fault distribution information need to be extracted by means of observers.

In this thesis, it is assumed that there is no modeling uncertainty or, at least, even if there is, it can be handled by the robustness property of a relatively low-gain sliding-mode controller. On the other hand, a typical description for the system uncertainty caused by system faults can be represented with the model of the system in (3.2). Also, remember that, by means of an observer, the residual can be generated as defined in (3.6) and (3.7), Assuming **C** is a unity matrix and from (3.9), it follows that,

$$\begin{aligned} \dot{\mathbf{r}}(t) &= \dot{\mathbf{e}}(t), \\ &= (\mathbf{A}-\mathbf{L})\mathbf{e}(t) + \mathbf{R}\mathbf{f}(t), \end{aligned} \tag{4.24}$$

Rearranging (4.24),

$$\mathbf{R}\mathbf{f}(t) = \dot{\mathbf{r}}(t) - (\mathbf{A}-\mathbf{L})\mathbf{e}(t). \tag{4.25}$$

Extracted fault information can be embedded into sliding mode controllers in two possible approaches in order to obtain a reconfiguring controller, which is robust to any system faults.

- Fault distribution information can be utilized in adjusting the corrective control part of sliding-mode controller.
- Fault distribution information can be inserted into equivalent control part of sliding-mode controller output.

4.4. Reconfiguring Controller Design

The reconfigurable controller proposed here is a modified version of standard sliding-mode controller. Sliding-mode controller is robust to model uncertainties when the upper boundary of the uncertainty is given. Assume there is no information for the upper boundary of the uncertainty caused by model mismatch or a system fault. In that case, the proposed methodology replaces corrective gain vector with fault distribution information or inserts the fault distribution information into equivalent control part of sliding mode controller to achieve the acceptable performance criteria.

4.4.1. First Approach: Switching-Gain Sliding-Mode Control

Consider a general linear MIMO system of the form in (3.2). In order to achieve all states of the system in (3.2) to track the given desired trajectories at the same time, the sliding manifold is defined as follows [3],

$$\mathbf{s}(t) = \tilde{\mathbf{x}}(t) + \Lambda \int \tilde{\mathbf{x}}(t)dt \tag{4.26}$$

where $\mathbf{s}$ is the sliding surface vector, Λ is a diagonal matrix which defines the slopes of the sliding surfaces, $\tilde{\mathbf{x}}$ is the state error vector and defined as,

$$\tilde{\mathbf{x}} = \mathbf{x} - \mathbf{x}_d \tag{4.27}$$

In order to guarantee stability, a candidate Lyapunov function is given in terms of sliding manifold given in (4.26)

$$\mathbf{V}(\mathbf{s}) = \frac{\mathbf{s}^T\mathbf{s}}{2}, \tag{4.28}$$

If the control satisfies the negative definiteness of the time derivative of the Lyapunov function in (4.28) is guaranteed, then, the stability of the overall system is guaranteed. The

system representation with fault distribution information can be presented in terms of system and actuator faults as defined in (3.5)

$$\dot{\mathbf{x}} = \mathbf{A}_{fault}\mathbf{x}(t) + \mathbf{B}_{fault}\mathbf{u}(t) \tag{4.29}$$

First derivative of sliding surface function becomes

$$\dot{\mathbf{s}}(t) = \dot{\tilde{\mathbf{x}}}(t) + \Lambda\tilde{\mathbf{x}}(t) = 0 \tag{4.30}$$

The system representation can be inserted into (4.30) under the assumption that there exists no uncertainty,

$$\dot{\mathbf{s}}(t) = \mathbf{A}\mathbf{x}(t) + \mathbf{B}\mathbf{u}(t) - \dot{\mathbf{x}}_d(t) + \Lambda\tilde{\mathbf{x}}(t) \tag{4.31}$$

The best approximate of control law similar to (4.10) for the system with uncertainties turns out to be,

$$\hat{\mathbf{u}} = \mathbf{B}_{fault}^{-1}[-\mathbf{A}_{fault}\mathbf{x}(t) + \dot{\mathbf{x}}_d(t) - \Lambda\tilde{\mathbf{x}}(t)] \tag{4.32}$$

The overall control scheme together with corrective control gain becomes,

$$\mathbf{u} = \hat{\mathbf{u}} - \mathbf{B}_{fault}^{-1}\mathbf{k}\,\mathrm{sgn}(\mathbf{s}) \tag{4.33}$$

The condition for **k** can be obtained in a similar way defined in (4.13) by inserting (4.32) and (4.33) into (4.31) as follows,

$$\begin{aligned}\dot{\mathbf{s}}(t) &= \mathbf{A}\mathbf{x}(t) + \mathbf{B}\mathbf{B}_{fault}^{-1}[-\mathbf{A}_{fault}\mathbf{x}(t) + \dot{\mathbf{x}}_d(t) - \Lambda\tilde{\mathbf{x}}(t)] - \dot{\mathbf{x}}_d(t) + \Lambda\tilde{\mathbf{x}}(t) - \mathbf{B}\mathbf{B}_{fault}^{-1}\mathbf{k}\,\mathrm{sgn}(\mathbf{s}),\\ &= (\mathbf{A}\mathbf{x}(t) - \mathbf{B}\mathbf{B}_{fault}^{-1}\mathbf{A}_{fault}\mathbf{x}(t)) + (\mathbf{I} - \mathbf{B}\mathbf{B}_{fault}^{-1})(-\dot{\mathbf{x}}_d(t) + \Lambda\tilde{\mathbf{x}}(t)) - \mathbf{B}\mathbf{B}_{fault}^{-1}\mathbf{k}\,\mathrm{sgn}(\mathbf{s}).\end{aligned} \tag{4.34}$$

So that **k** must verify,

$$\mathbf{k} \geq \left\|\mathbf{B}^{-1}\mathbf{B}_{fault}\mathbf{A}\mathbf{x}(t) - \mathbf{A}_{fault}\mathbf{x}(t) + (\mathbf{B}^{-1}\mathbf{B}_{fault} - \mathbf{I})(-\dot{\mathbf{x}}_d(t) + \Lambda\tilde{\mathbf{x}}(t))\right\| + \eta\mathbf{B}^{-1}\mathbf{B}_{fault}, \tag{4.35}$$

If there exists uncertainty in system matrix but not in input matrix, in other words, if $\mathbf{B} = \mathbf{B}_{fault}$, then,

$$\mathbf{k} \geq \left\| \mathbf{A}\mathbf{x}(t) - \mathbf{A}_{fault}\mathbf{x}(t) + (\mathbf{I} - \mathbf{I})(-\dot{\mathbf{x}}_{\mathbf{d}}(t) + \Lambda\tilde{\mathbf{x}}(t)) \right\| + \eta\mathbf{I}, \tag{4.36}$$

Hence,

$$\mathbf{k}_{fault} \geq \mathbf{R}\mathbf{f}(t) + \eta, \tag{4.37}$$

The corrective gain vector $\mathbf{k}$ in (4.33) is replaced with fault distribution information for faulty case and a nominal gain vector is used for nominal case. In case a fault is detected by means of FD scheme, then the corrective controller gain vector is switched to fault distribution vector as shown below.

$$\mathbf{k} = \begin{cases} \mathbf{k}_{nom} = \eta & \text{for nominal plant} \\ \mathbf{k}_{fault} = \mathbf{R}\mathbf{f} + \eta & \text{for faulty plant} \end{cases} \tag{4.38}$$

In other words the fault distribution vector is taken as the corrective control gain vector of standard sliding-mode controller. The desired trajectories given in Figure 4.5 are required to be achieved by the controller.

The trajectory task performance has been achieved for both outputs of MIMO system with the proposed reconfiguring controller scheme, which uses sliding-mode controller as the baseline controller [9]. Here, the fault or uncertainty information is extracted from the system dynamics by means of an observer and embedded into corrective control part of reconfiguring sliding mode controller scheme. A soft nonlinear switching function is used to avoid chattering for the nominal plant.

The system fault is detected by comparing any component of residual vector with any corresponding scalar threshold component which is found by trial and error in a similar way defined in (3.19).

4.4.1.1. Design Example and Simulations for First Approach. Consider state-space representation of a MIMO system in (3.28), a system fault is inserted into the system matrix **A** consequently, the state space representation of the faulty system became as defined in (3.29). The eigenvalues change as defined in (3.30) for nominal plant to eigenvalues defined in (3.31) for faulty plant. The fault is easy to detect but difficult to control after the eigenvalue changes due to fault.

The fault information within fault distribution matrix will be obtained as follows [47, 48],

$$\begin{aligned}\mathbf{Rf}(t) &= \dot{\mathbf{r}}(t) - (\mathbf{A}-\mathbf{L})\mathbf{e}(t), \\ &= \dot{\mathbf{r}}(t) - \left\{\begin{bmatrix}-2 & 0.1\\ 2 & 3\end{bmatrix} - \begin{bmatrix}21 & -17.9\\ 1692 & 21\end{bmatrix}\right\}\begin{bmatrix}\tilde{x}_1\\ \tilde{x}_2\end{bmatrix}, \\ &= \begin{bmatrix}\dot{r}_1 + 23\tilde{x}_1 - 0.1\tilde{x}_2\\ \dot{r}_2 + 2\tilde{x}_1 + 18\tilde{x}_2\end{bmatrix}\end{aligned} \tag{4.39}$$

Each fault distribution vector term has been used as the corrective control gain vector of standard sliding-mode controller as defined in (4.37) and (4.38). In other words, the controller transformed to run in an adaptive manner in case a fault detected in the system dynamics. Matlab-SIMULINK software has been used for simulations. A bias system fault as defined in Chapter 3.4.2.2. inserted at 1.25 sec. into the nominal system and this fault has been removed at 1.75 sec. of the simulation. Following desired trajectories given in Figure 4.9 are required to be achieved by the controller.

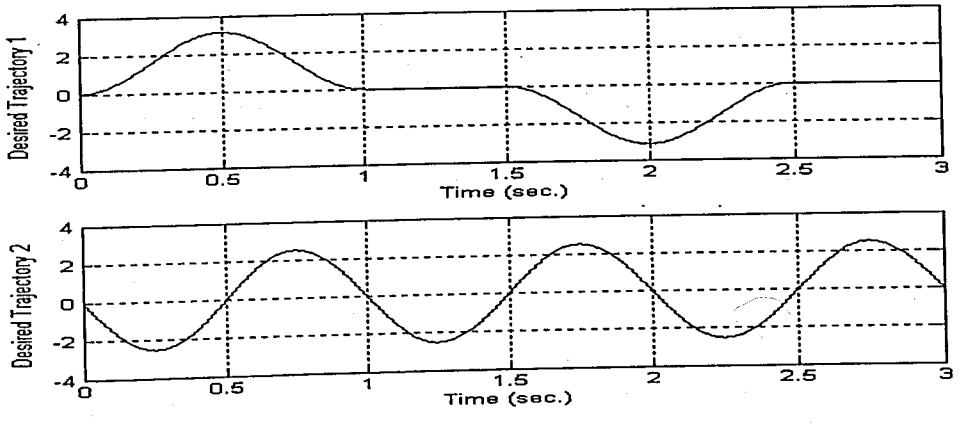

Figure 4.9. Desired trajectories [48]

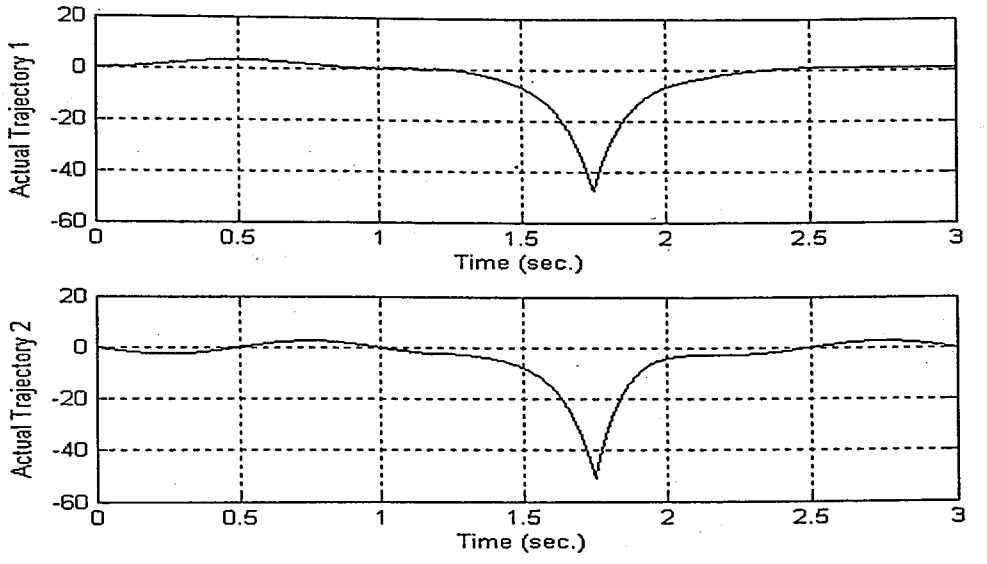

Figure 4.10. Actual trajectories with standard sliding-mode scheme [48]

It is observed that the standard sliding mode controller cannot cope with the structured (or parametric) uncertainties [20] inserted into the system as a result of the system fault. It is seen from Figure 4.10 that the magnitude of the fault would grow unboundedly if the system has not been simulated to act nominally. On the other hand proposed controller scheme copes with the fault and stops system dynamics to wind-up.

It is also observed from Figure 4.11 that the control inputs are out of realistic values during the faulty period. This illustrates the fact that the fault had adverse effect on the system dynamics and therefore the reconfiguration of the controller is essential.

First approach of proposed scheme which inserts fault distribution information into corrective control part of reconfiguring sliding mode controller shows better performance when compared with standard sliding mode controller as can be seen in Figure 4.12. The trajectory following is not perfect but the system is still in operation.

The activity of the reconfigured controller under the faulty condition can be seen in Figure 4.13 clearly. Note, the control activity is considerably higher during the faulty situation, whereas it is reduced under nominal condition.

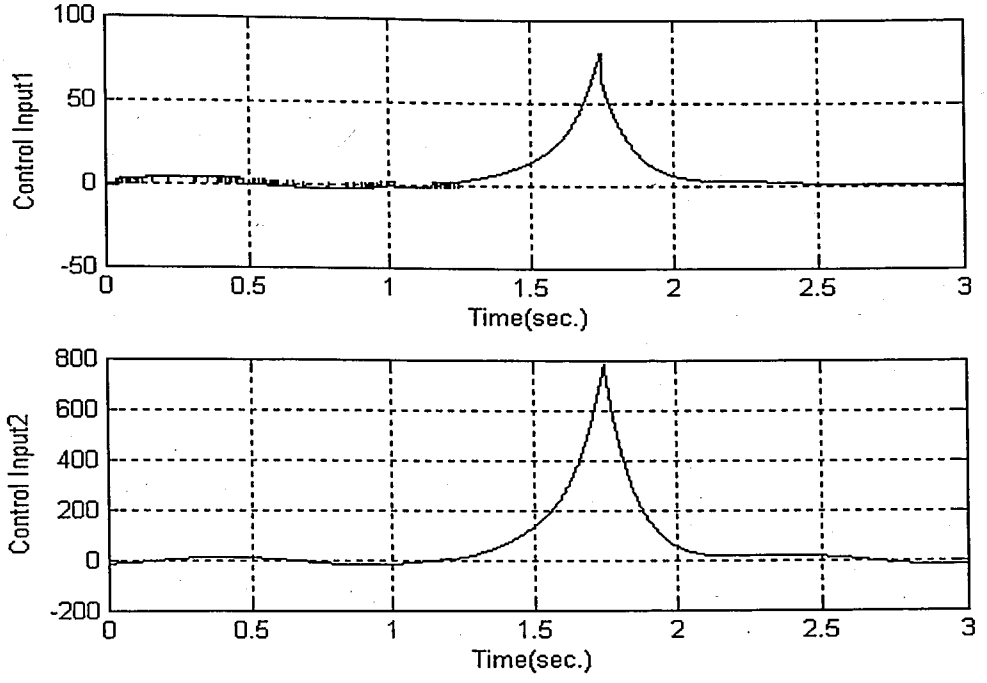

Figure 4.11. Control inputs with standard sliding-mode scheme [48]

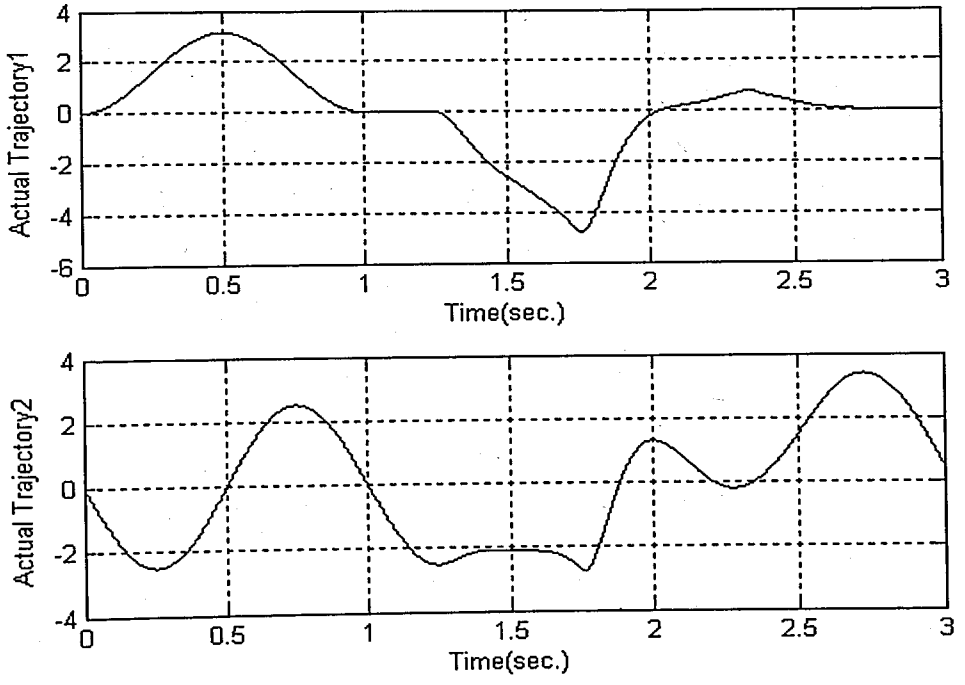

Figure 4.12. Actual trajectories with first approach of reconfiguring controller scheme

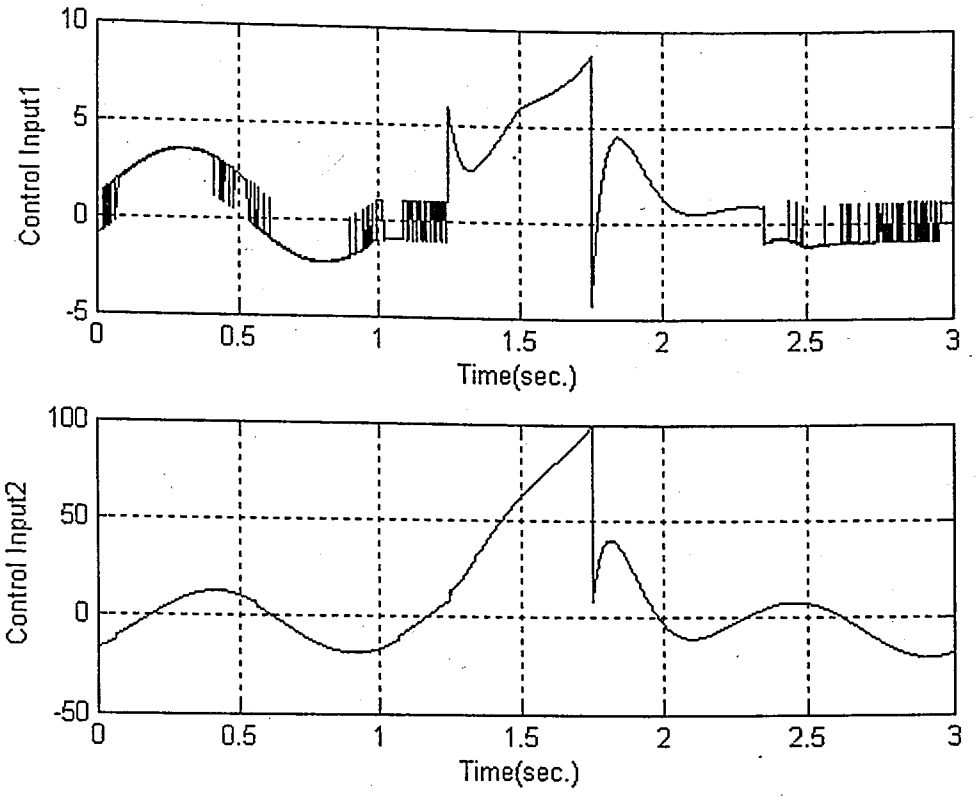

Figure 4.13. Controller inputs with first approach of reconfiguring controller scheme

4.4.2. Second Approach: Fault Information Inserted into Equivalent Control Part

Our second approach is based on the idea of updating the equivalent control part of the sliding-mode control action using the fault distribution information whenever a fault is detected.

It follows from (3.2) and (4.30), that the system representation with the fault distribution vector is inserted into (4.30)

$$\dot{\mathbf{s}}(t) = \mathbf{A}\mathbf{x}(t) + \mathbf{B}\mathbf{u}(t) + \mathbf{R}\mathbf{f}(t) - \dot{\mathbf{x}}_d(t) + \Lambda\tilde{\mathbf{x}}(t) \tag{4.40}$$

hence, the equivalent control term is obtained as

$$\mathbf{u}_{eq}(t) = \mathbf{B}^{-1}\left[-\mathbf{A}\mathbf{x}(t) - \mathbf{R}\mathbf{f}(t) + \dot{\mathbf{x}}_d(t) - \Lambda\tilde{\mathbf{x}}(t)\right]. \tag{4.41}$$

It is clear that all terms are known except fault distribution matrix in (4.38). To satisfy the sliding condition a corrective control term is used for sliding mode controllers. The overall controller with the corrective control term will be derived as,

$$\mathbf{u}(t) = \mathbf{u}_{eq}(t) - \mathbf{B}^{-1}[\mathbf{k}_{nom} sat(\frac{\mathbf{s}}{\Phi})]. \tag{4.42}$$

where $\mathbf{k}_{nom}$ is the corrective gain vector which is also used for nominal case to guarantee a sliding regime on the switching surface vector **s**. As the fault distribution vector $\mathbf{CRf}(t)$ term inserted into the equivalent control part of controller scheme, the controller runs in a reconfiguring adaptive manner and makes it possible to accommodate with system faults.

Proposed second approach of reconfiguring sliding mode controller copes satisfactorily with the mentioned uncertainties by updating the equivalent control part of reconfiguring sliding mode controller as can be seen from Figure 4.14 and Figure 4.15. Note that the control activity increases under faulty situation. In return, fault tolerant control is accomplished with reconfiguring sliding mode controller.

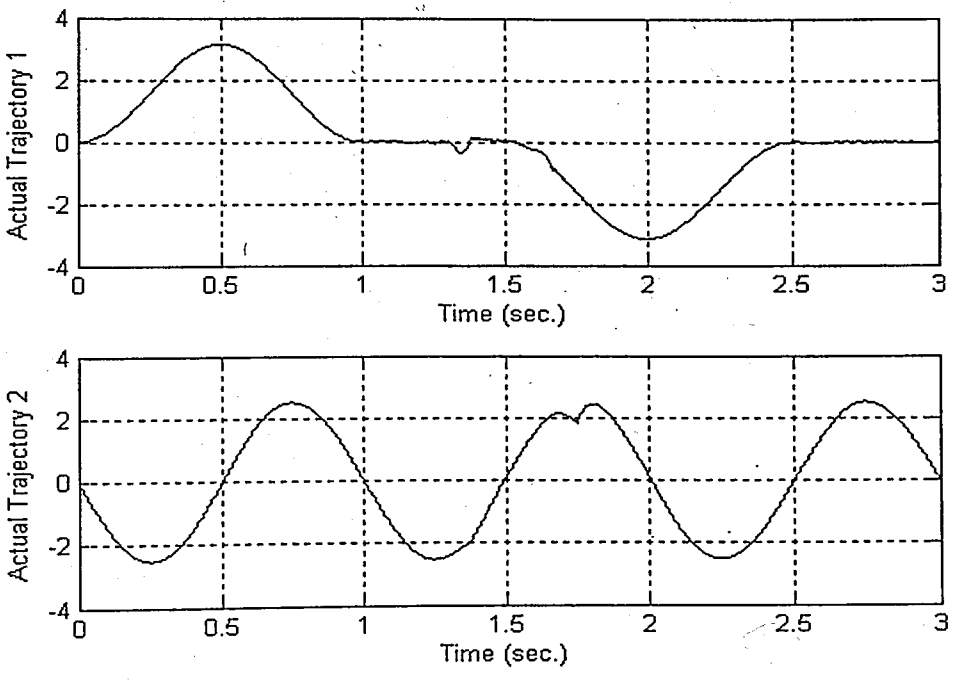

Figure 4.14. Actual trajectories with second approach of reconfiguring controller scheme [48]

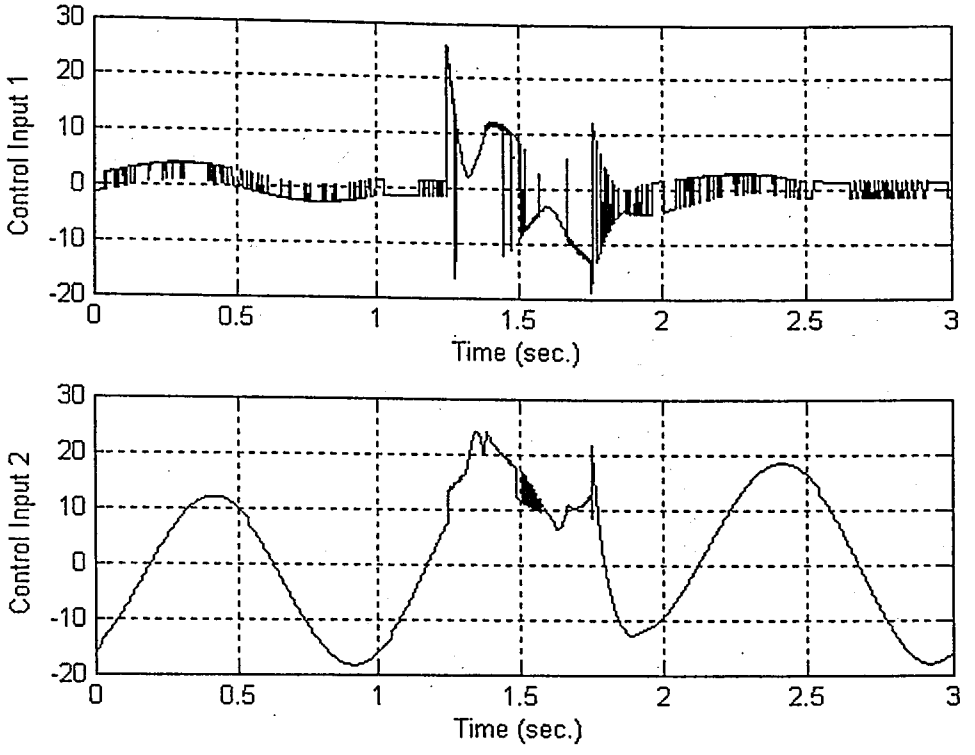

Figure 4.15. Controller inputs with second approach of reconfiguring controller scheme [48]

4.5. Discussions

A reconfiguring sliding mode controller is proposed for linear MIMO systems. Reconfiguring controller alleviates the disturbances inserted into the system dynamics in case of a fault by reconfiguring the equivalent control term or corrective gain vector term of the sliding mode controller in an adaptive manner. It is observed that the standard sliding mode controller cannot cope with uncertainties due to system fault. On the other hand, the switching gain reconfiguration can cope with faulty condition much better than the standard sliding-mode controller and stops system dynamics to wind-up at the faulty situation. Second approach can also cope with mentioned uncertainties by updating the equivalent control part of a sliding-mode controller with respect to fault distribution information. In fact, by comparing Figure 4.12 and 4.14, it is seen that updating the equivalent control term yields better performance as compared to a switched gain controller.

The algorithm based on the extraction of fault distribution information from system dynamics by means of a linear observer. This method is an example for the integration of fault detection methods with robust control techniques to obtain fault tolerant control. The proposed controller schemes can be seen as active reconfiguration methods. This method can be implemented for the control of underwater and aerospace vehicles especially when there is no way to terminate the process and fix the faulty system component.

5. SIMULATION RESULTS

The proposed control reconfiguration scheme is implemented for the depth control of the submarine. Our aim is to keep the vehicle at submergence in order to avoid detection by surface units in case of approaching to surface as a result of forces and moments acting on the submarine.

5.1. Re-Configuring Sliding-Mode Controller Design

The controller is designed in a way similar to MIMO linear model defined in Chapter 4. Submarine dynamics is reduced to two-input-two-state form by treating pitch angle $\theta(t)$ as a known disturbance and computing the auxiliary tank content $M_{e_{aux}}$ a priori separate from hydroplane inputs. Reduced state space model of the submarine dynamics turns out to be [52],

$$\dot{\mathbf{x}}_n(t) = \mathbf{A}_n\mathbf{x}_n(t) + \mathbf{B}_n\mathbf{u}(t) + \mathbf{R}_n\mathbf{d}(t) + \mathbf{F}\theta(t) \tag{5.1}$$

where

$$\mathbf{x}_n(t) = \begin{bmatrix} w(t) \\ Q(t) \end{bmatrix} \text{ and } \mathbf{u}(t) = \begin{bmatrix} \delta B(t) \\ \delta S(t) \\ M_{e_{aux}} \end{bmatrix}$$

and, it follows from (2.4) and (5.1),

$$\mathbf{A}_n = \begin{bmatrix} -0.0245313 & 1.5174 \\ 0.0003372 & -0.0771345 \end{bmatrix} \quad \mathbf{B}_n = \begin{bmatrix} 0.046192185 & -0.079592688 \\ 0.000479688 & -0.002184535 \end{bmatrix},$$

$$\mathbf{F} = \begin{bmatrix} 0.0162 & 0 \\ 0 & -0.003975 \end{bmatrix}.$$

For the system in (5.1), the state estimates $\hat{\mathbf{x}}_n(t)$ can be generated by means of a Luenberger observer, as

$$\dot{\hat{\mathbf{x}}}_n(t) = (\mathbf{A}_n - \mathbf{L})\hat{\mathbf{x}}_n(t) + \mathbf{B}_n\mathbf{u}(t) + \mathbf{F}\theta(t) + \mathbf{L}\mathbf{x}_n(t), \tag{5.2}$$

Defining the state estimation error as in (4.24), its dynamics can be written from (5.1) and (5.2)

$$\begin{aligned} \dot{\mathbf{e}}(t) &= \dot{\mathbf{x}}_n(t) - \dot{\hat{\mathbf{x}}}_n(t), \\ &= (\mathbf{A}_n - \mathbf{L})\mathbf{e}(t) + \mathbf{R}_n\mathbf{d}(t), \end{aligned} \tag{5.3}$$

From (5.4), disturbance information can be extracted similar to (4.26) as [52],

$$\mathbf{R}_n\mathbf{d}(t) = \dot{\mathbf{e}}(t) - (\mathbf{A}_n - \mathbf{L})\mathbf{e}(t) \tag{5.4}$$

It is known that a sliding-mode controller can be made robust to uncertainties in system dynamics when the upper bound of the uncertainty is given [26]. For the proposed methodology below, no information for the upper bound of the uncertainty (which may be caused by a model mismatch or disturbances) is necessary since the disturbance information obtained in (5.4) is used as an additive term in the corrective or equivalent control part of the control action.

In order to achieve all states of the system in (5.1) to track the given desired trajectories at the same time, the switching surface function [53] can be defined. Similar methodology defined in (4.33)-(4.42) can be implemented and the control law can be obtained in two approaches explained in Chapter 3.

5.1.1. First Approach: Modified Corrective Control Term

The first approach is to use extracted disturbance distribution information as an additive term to the corrective control part of the controller. From (4.31) and (5.1) without uncertainty information, it follows that

$$\dot{\mathbf{s}}(t) = \mathbf{A}_n \mathbf{x}_n(t) + \mathbf{B}_n \mathbf{u}(t) + \mathbf{F}\theta(t) - \dot{\mathbf{x}}_d(t) + \Lambda\tilde{\mathbf{x}}(t), \tag{5.5}$$

Rearranging (5.5),

$$\mathbf{B}_n \mathbf{u}_{eq} = -\mathbf{A}_n \mathbf{x}_n(t) - \mathbf{F}\theta(t) + \dot{\mathbf{x}}_d - \Lambda\tilde{\mathbf{x}}(t) \tag{5.6}$$

or

$$\mathbf{u}_{eq}(t) = \mathbf{B}_n^{-1}\left[-\mathbf{A}_n \mathbf{x}_n(t) - \mathbf{F}\theta(t) + \dot{\mathbf{x}}_d(t) - \Lambda\tilde{\mathbf{x}}(t)\right]. \tag{5.7}$$

Corrective control term can be added similar to (4.36) and (4.38), and, the overall reconfiguring sliding-mode controller turns out to be,

$$\mathbf{u}(t) = \mathbf{u}_{eq}(t) - \mathbf{B}^{-1}[(\mathbf{k})sat(\frac{\mathbf{s}}{\Phi})] \tag{5.8}$$

where

$$\mathbf{k} = \begin{cases} \mathbf{k}_{nom} = \eta, & \text{for nominal plant} \\ \mathbf{k}_{fault} = \mathbf{R}_n \mathbf{d}(t) + \eta, & \text{for faulty plant} \end{cases}$$

and η is a positive definite vector for the nominal plant. Here, $\mathbf{R}_n\mathbf{d}$ can be replaced by its estimate obtained from (5.4).

Simulations are performed with Matlab-SIMULINK software. Desired depth trajectory is defined in the following way. The depth velocity of the submarine is given as,

$$\dot{h}(t) = w(t)\cos\theta(t) - U\sin\theta(t) \tag{5.9}$$

For small angles, the desired depth dynamics can be written as

$$\dot{h}_d(t) = w_d(t) - U\theta_d(t) \tag{5.10}$$

which is a combination of desired heave velocity w_d and desired pitch angle θ_d. The desired pitch angle trajectory is chosen to be 0° during the simulation, then, the desired heave velocity dynamics turns out to be

$$w_d(t) = \dot{h}_d(t) \tag{5.11}$$

So, the desired heave velocity can be obtained by differentiating the profile of desired depth h_d. During the simulations, the depth profile given in Figure 5.1 is used, which corresponds to a diving maneuver from the sea level to a depth of 30 ft (10 m).

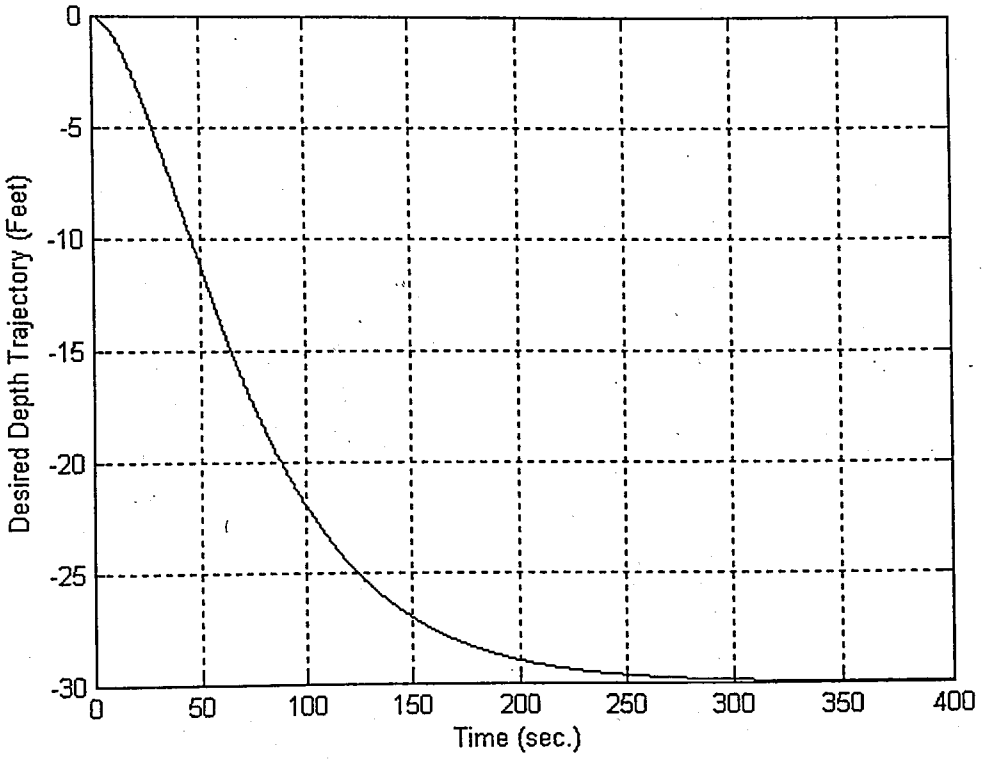

Figure 5.1. Desired depth trajectory [51]

Firstly, a standard sliding-mode controller is designed for the depth control of the submarine is designed based on the nominal plant where the disturbances are not taken into account. It performs unsatisfactorily which can be seen in Figure 5.2. which shows that the submarine cannot leave the sea surface because of the suction force.

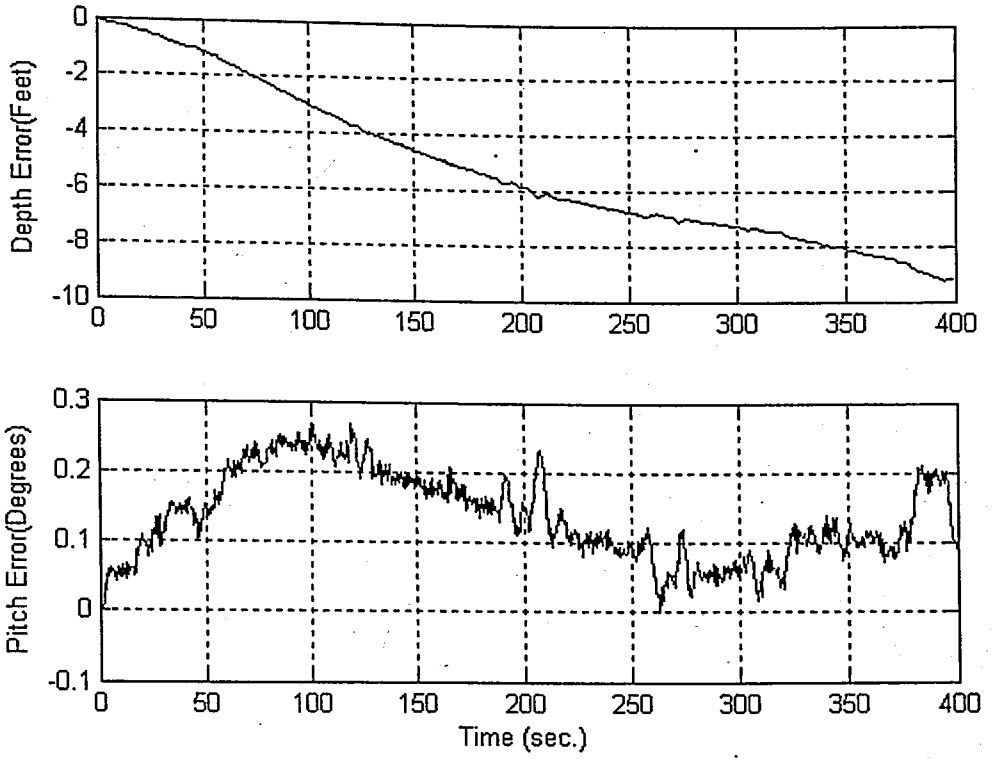

Figure 5.2. Depth and pitch error values for sea state 6 with standard scheme [52]

An indirect adaptive controller is designed in order to investigate the performance of adaptive controllers under system faults with the same submarine model. It has been observed that the indirect adaptive controller, which the parameters of the controller are updated with respect to estimated system coefficients also cannot cope with disturbances at sea state 6 [19]. Indirect self-tuning control technique is applied to the depth and pitch angle control of the same submarine model in case of system faults in order to perform active reconfiguration. Satisfactory results obtained for sea state 1 but the performance degraded when the effects of the sea waves increased in case of sea state 6.

Parameter estimation for time-varying parameters due to sea wave and system fault effects is performed with RLS algorithm. Estimated parameters converged to true parameters of the submarine model for sea state 1. Same forgetting factor 0.98 has been used throughout the simulations. Forgetting factor is defined by trial and error. Fault detection is not required but performed by using parameter estimation algorithm. It has been observed that the parameters of the system dynamics change rapidly and inputs of recursive least square (RLS) estimation with forgetting factor are not persistently enough

in order to converge to the true parameters of changed system dynamics due sea state 6 sea wave effects.

In our approach, firstly, each disturbance distribution vector term has been inserted into the standard sliding-mode controller as an additive gain for the corrective control part as can be seen in (5.8). In other words, the controller is adapted to the changes in system dynamics from the corrective control part whenever there is a change in sea states. In other words, submarine states are continuously observed. The submarine depth control for sea state 1 situation with respect to a given desired trajectory up to 30 ft (10 m) depth is performed with the proposed sliding mode control scheme and the results are evaluated.

The desired and actual depth outputs are shown together in Figure 5.3 and depth and pitch angle errors are shown in Figure 5.4 for sea state 1 when the effects of sea waves on the submarine is relatively small. It looks like that there is excessive chattering on the control planes when the control commands are observed in Figure 5.5. Depth and pitch error values are satisfactory (less than 0.6 ft - 20 cm -) as can be seen in Figure 5.4.

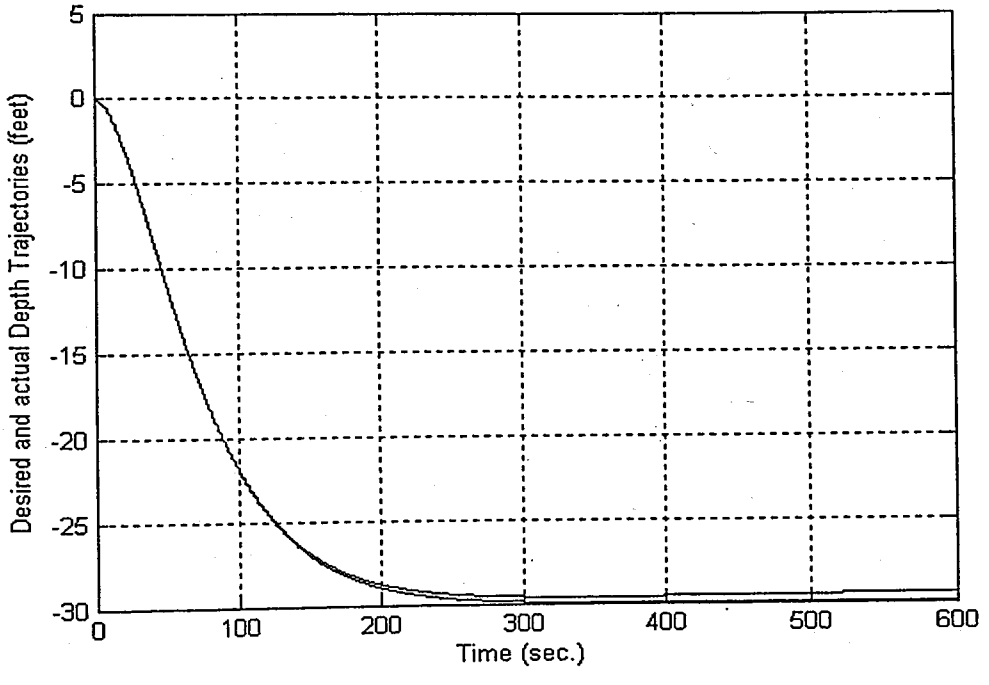

Figure 5.3. Desired and actual depth trajectories for sea state 1 with switching gain sliding-mode controller

It can be clearly seen that the depth error cannot converge to zero as the error trajectory shows an increasing pattern in Figure 5.4. This is not the case when the same approach is implemented for sea state 6.

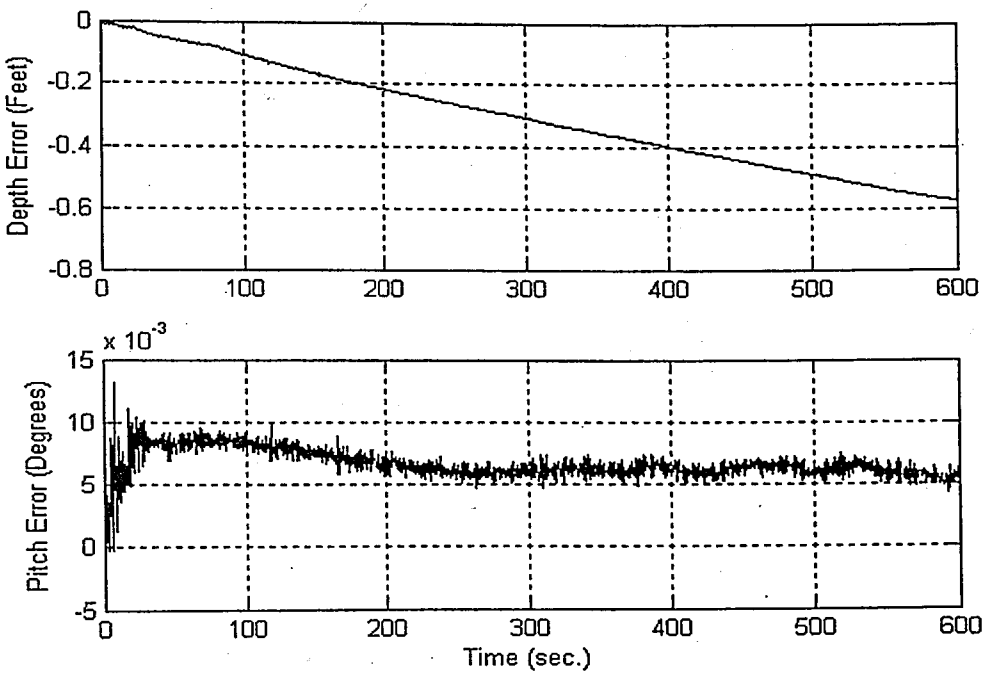

Figure 5.4. Depth and pitch errors for sea state 1 with switching gain sliding-mode controller

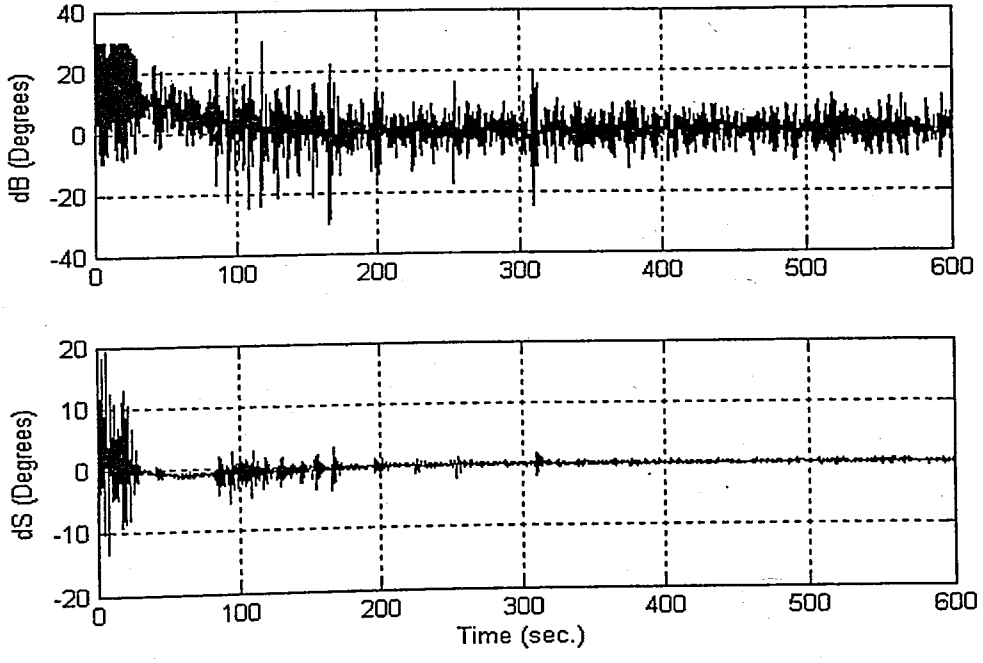

Figure 5.5. Bow and stern plane commands for sea state 1 with switching gain sliding-mode controller

The same scenario is simulated also with sea state 6. Sea state 6 is the limit for almost all vessels on the sea therefore, simulation results at this sea state are particularly important. The desired and actual depth outputs are shown together in Figure 5.6 and depth and pitch angle errors are shown in Figures 5.7 and 5.8 for sea state 6 when the effects of sea waves on the submarine is huge.

It looks like that there is excessive chattering on the control planes when the control commands are observed in Figure 5.9.

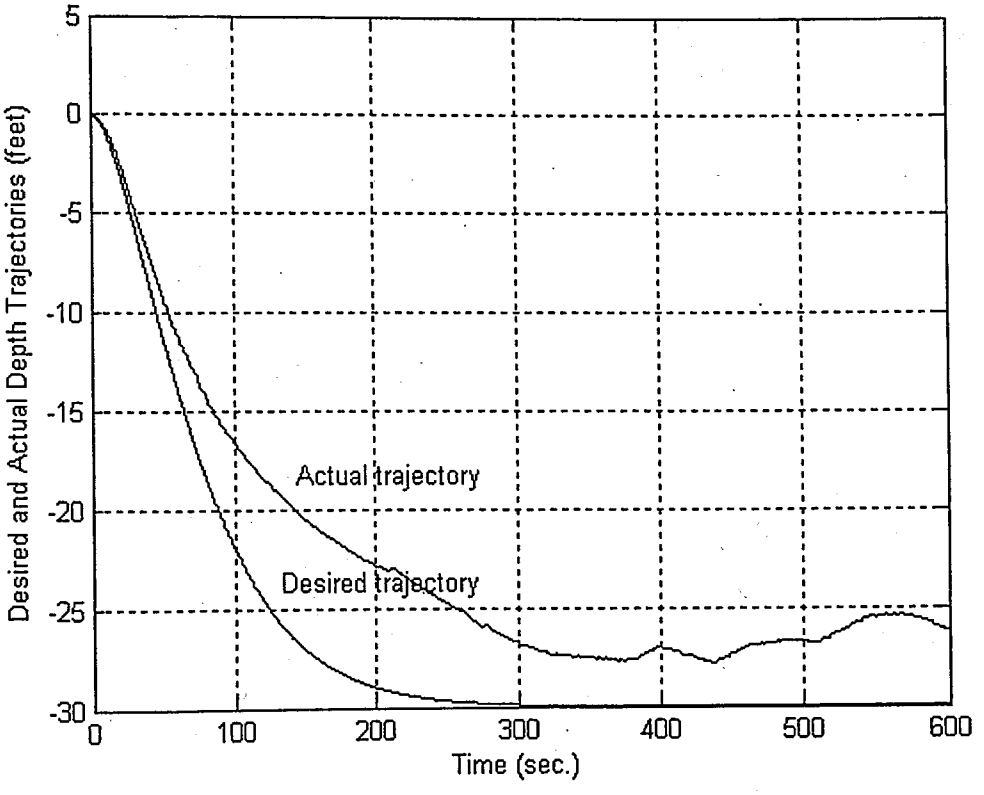

Figure 5.6. Desired and actual depth trajectories for sea state 6 with switching gain sliding-mode controller

Depth and pitch error values are greater than the simulation results depicted for sea state 1 (maximum 6.5 ft - 2 m -) as can be seen in Figure 5.7 and 5.8. The control activity for duration of 5 seconds is shown in Figure 5.10, where it can be seen that the variation of the control action is within implementable limits. As compared to the sea state 1 scenario control inputs increase and the saturation of the bow plane inputs causes an increase and

saturation for the stern plane inputs. However, the response shown in Figure 5.5 is still within acceptable limits.

That means, the proposed scheme of updating corrective control part of sliding-mode controller in an adaptive manner can compensate adverse sea affects to some degree. Note that, standard sliding-mode and adaptive controllers cannot cope with disturbances in case of sea state 6. But, our switching gain sliding-mode controller gives better performance than standard sliding-mode and adaptive controllers.

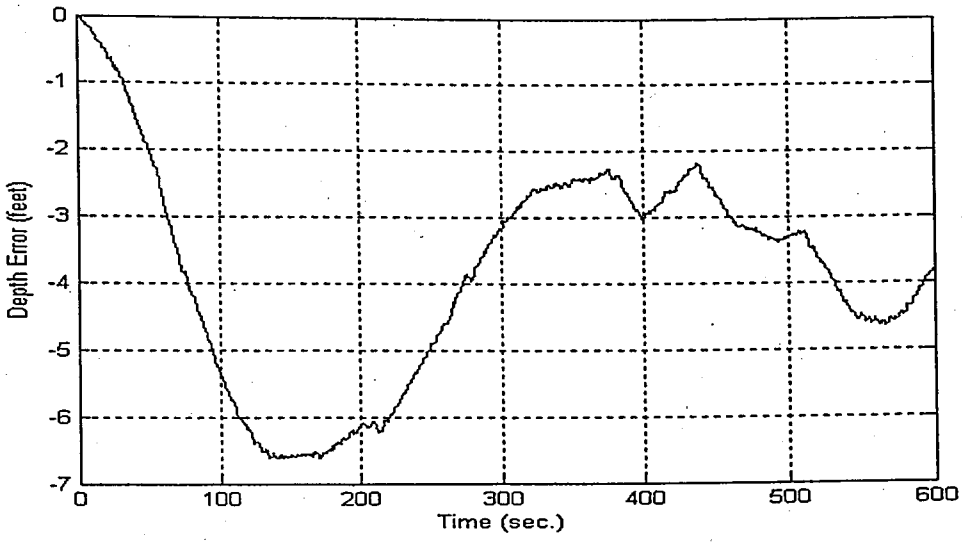

Figure 5.7. Depth error for sea state 6 with switching gain sliding-mode controller

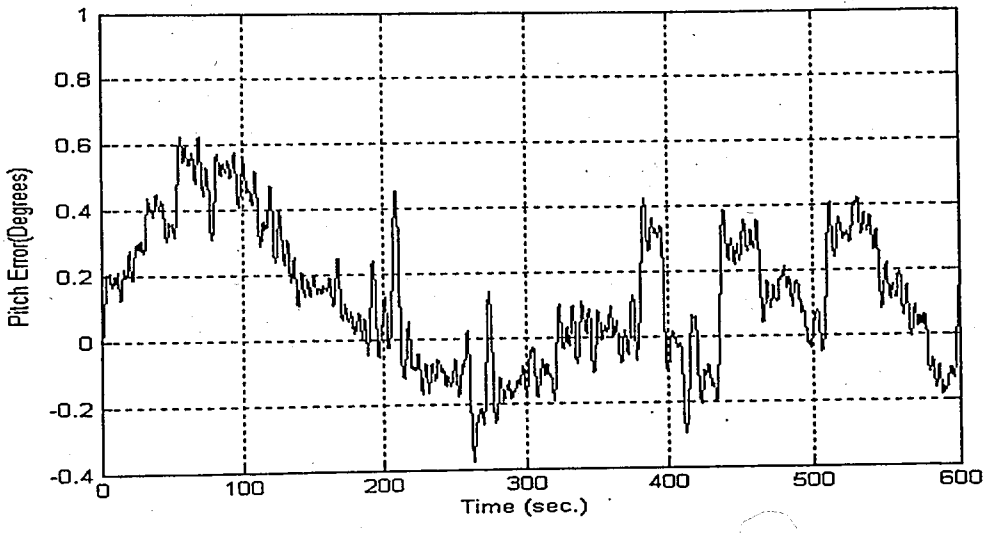

Figure 5.8. Pitch error for sea state 6 with switching gain sliding-mode controller

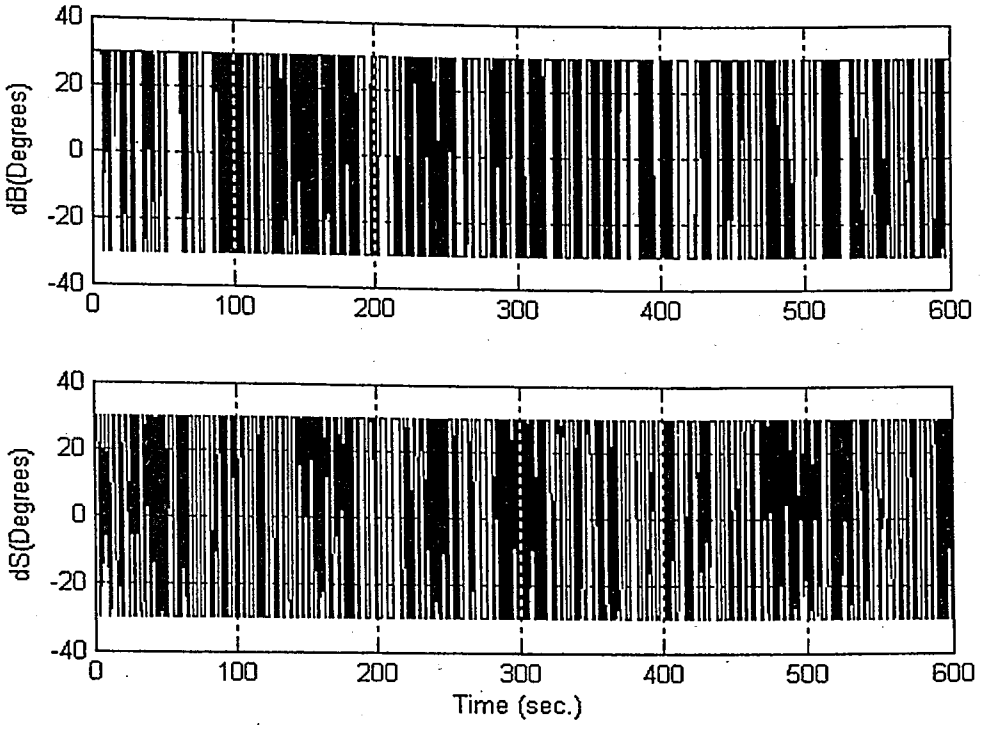

Figure 5.9. Bow and stern plane commands for sea state 6 with switching gain sliding-mode controller

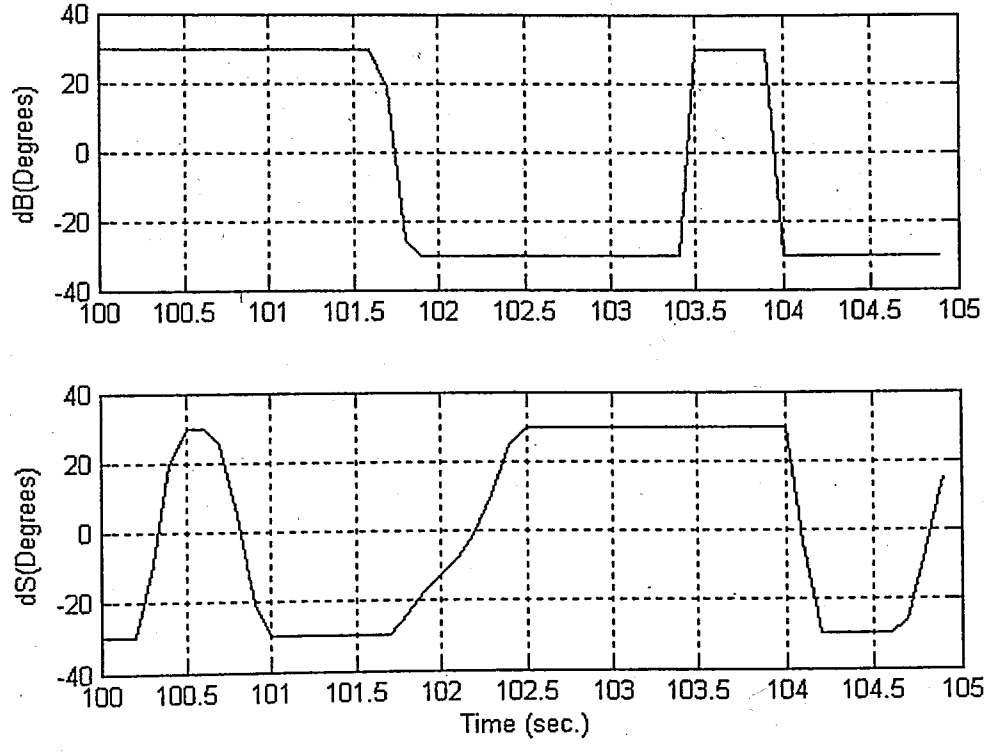

Figure 5.10. Bow and stern plane commands for sea state 6 in a smaller scale with switching gain sliding-mode controller

5.1.2. Second Approach: Modified Equivalent Control Term

The second approach is to use extracted disturbance distribution information as an additive term to equivalent control part of the controller, it follows the same approach defined in (3.40), from (5.1) and (5.4) [52],

$$\dot{\mathbf{s}}(t) = \mathbf{A}_n \mathbf{x}_n(t) + \mathbf{B}_n \mathbf{u}(t) + \mathbf{R}_n \mathbf{d}(t) + \mathbf{F}\theta(t) - \dot{\mathbf{x}}_d(t) + \Lambda\tilde{\mathbf{x}}(t), \tag{5.12}$$

Rearranging (5.12),

$$\mathbf{B}_n \mathbf{u}_{eq} = -\mathbf{A}_n \mathbf{x}_n(t) - \mathbf{R}_n \mathbf{d}(t) - \mathbf{F}\theta(t) + \dot{\mathbf{x}}_d - \Lambda\tilde{\mathbf{x}}(t) \tag{5.13}$$

or

$$\mathbf{u}_{eq}(t) = \mathbf{B}_n^{-1}\left[-\mathbf{A}_n \mathbf{x}_n(t) - \mathbf{R}_n \mathbf{d}(t) - \mathbf{F}\theta(t) + \dot{\mathbf{x}}_d(t) - \Lambda\tilde{\mathbf{x}}(t)\right]. \tag{5.14}$$

In this approach, each disturbance distribution vector term has been inserted into the standard sliding-mode controller as an additive term for the equivalent control part as can be seen in (5.14). In other words, the controller is adapted to the system dynamics from the equivalent control part whenever there is a change in sea states. The submarine depth control for sea state 1 situation with respect to a given desired trajectory up to 30 ft (10 m) depth is performed with the proposed sliding mode control scheme and the results are evaluated.

It looks like that there is excessive chattering on the control planes when the control commands are observed in Figure 5.11. This is not true if a shorter duration of the hydroplane activity is taken into account. It can be seen in Figure 5.12, which shows the control activity detail of 5 seconds that the variation of control action is acceptable and implementable. Depth and pitch error values are much better than being just satisfactory (less than 0.025 ft - 0.75 cm -) as can be seen in Figure 5.13.

The same scenario is simulated also with sea state 6. The control activity for a duration of 5 seconds is shown in Figure 5.14, where it can be seen that the variation of the control action is within implementable limits. As compared to the sea state 1 scenario control inputs increase and the saturation of the bow plane inputs causes an increase and saturation for the stern plane inputs. However, the response shown in Figure 5.15 is still within acceptable limits. Depth error is around 1 ft (30 cm) and pitch error is around 0.2°.

That means, the proposed second approach scheme reconfigures the controller structure in order to compensate adverse sea affects.

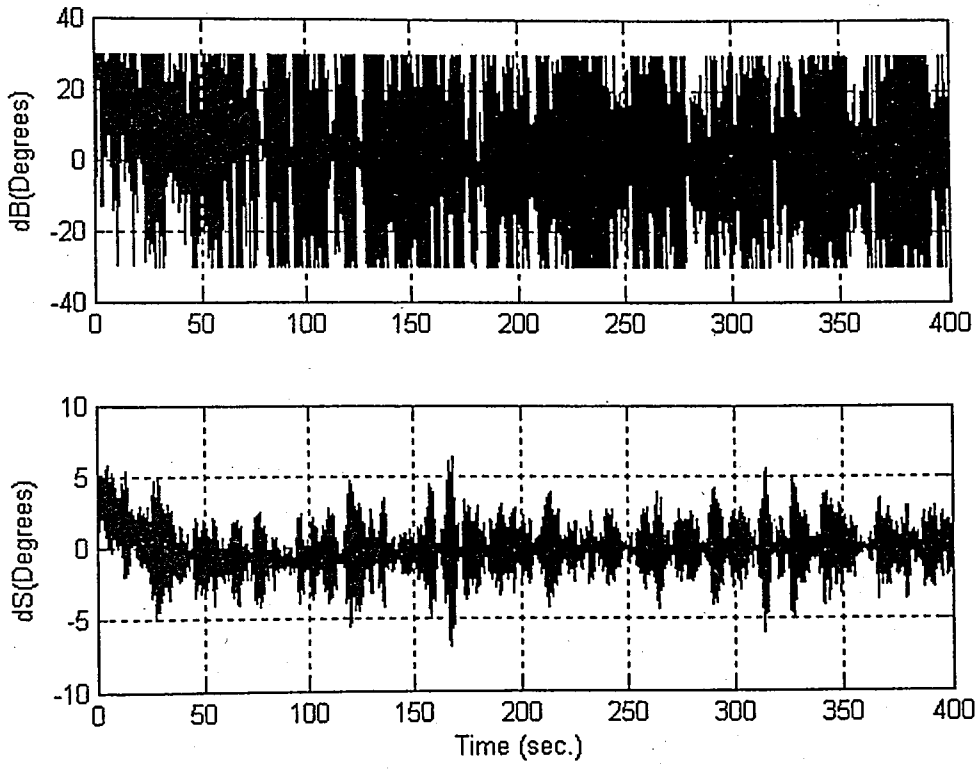

Figure 5.11. Bow and stern plane commands for sea state 1 with modified equivalent control part of a sliding-mode controller [52]

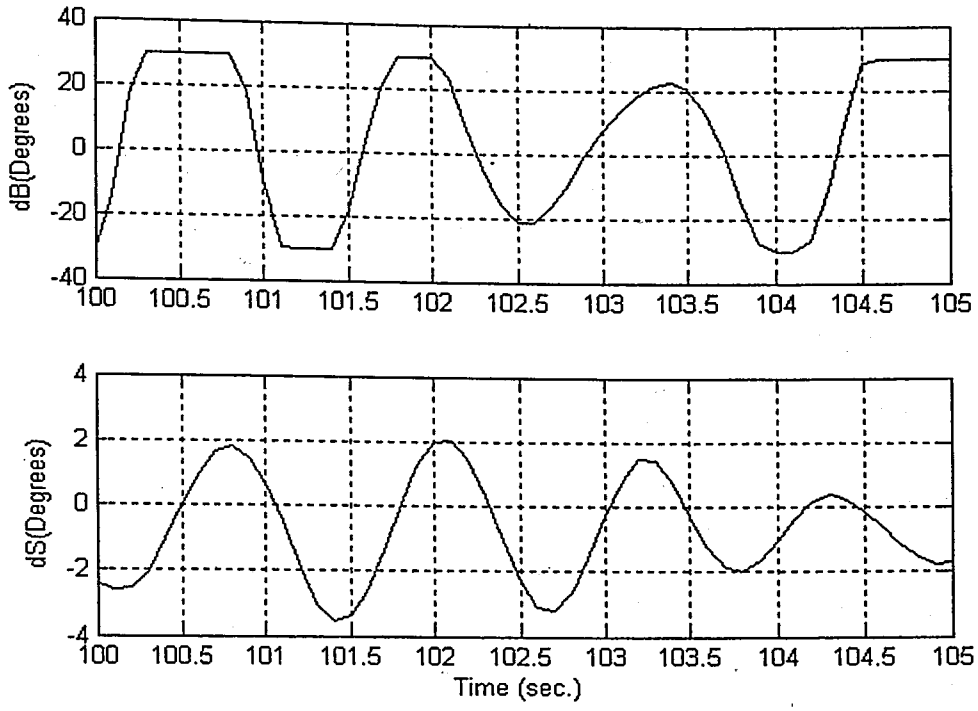

Figure 5.12. Bow and stern plane commands for sea state 1 in a smaller scale with modified equivalent control part of a sliding-mode controller [52]

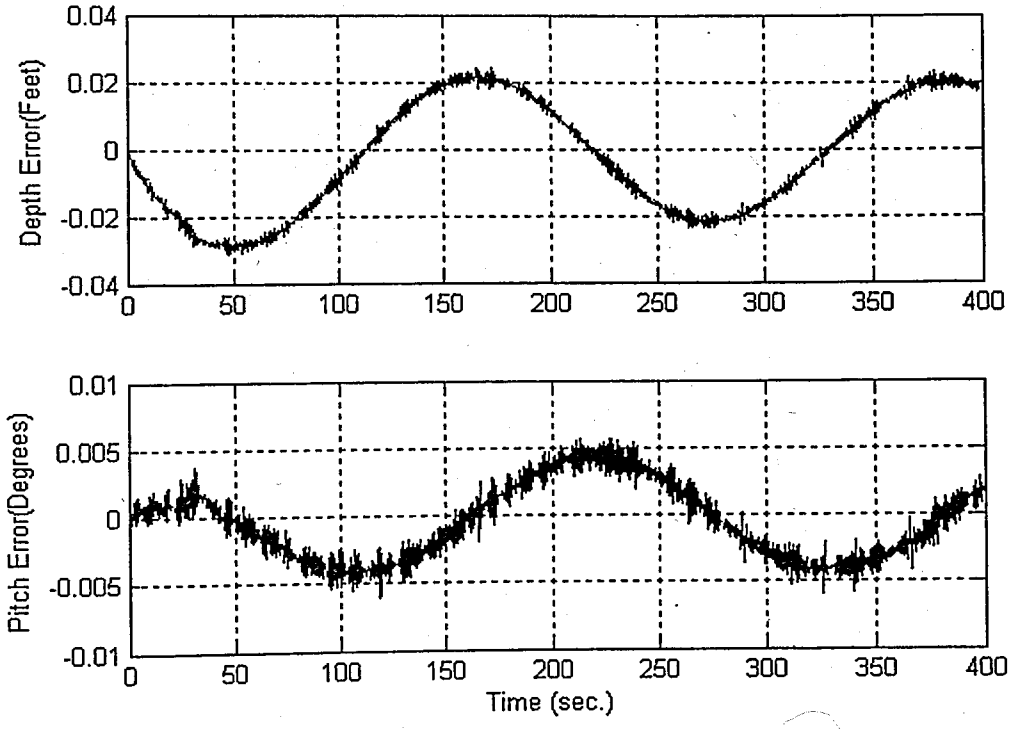

Figure 5.13. Depth and pitch error values for sea state 1 with modified equivalent control part of a sliding-mode controller [52]

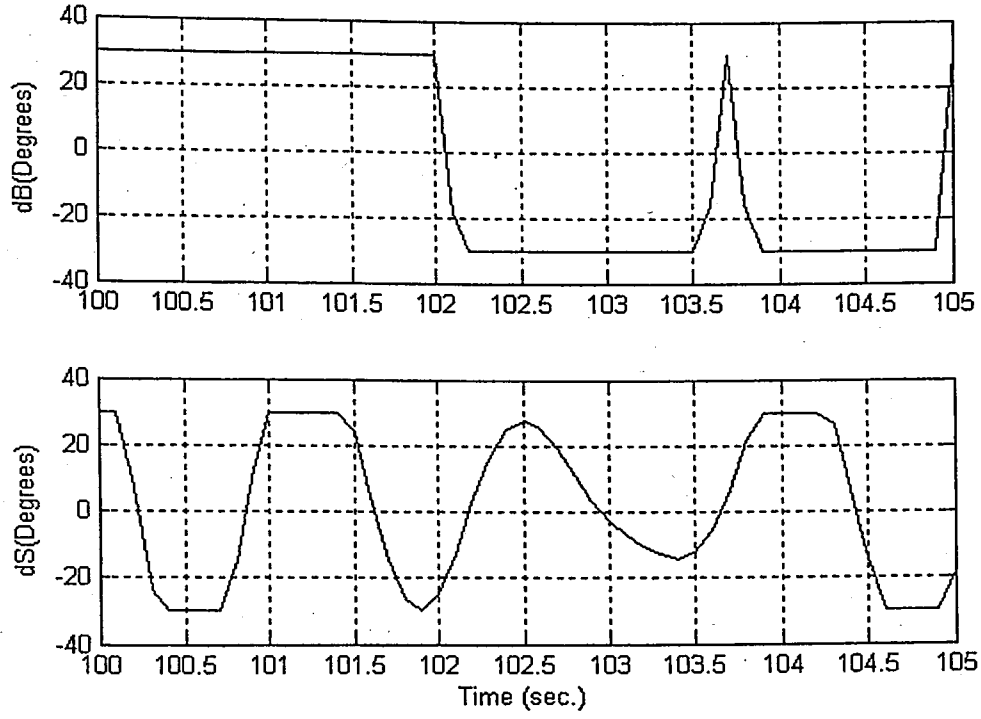

Figure 5.14. Bow and stern plane commands for sea state 6 in a smaller scale with modified equivalent control part of a sliding-mode controller [52]

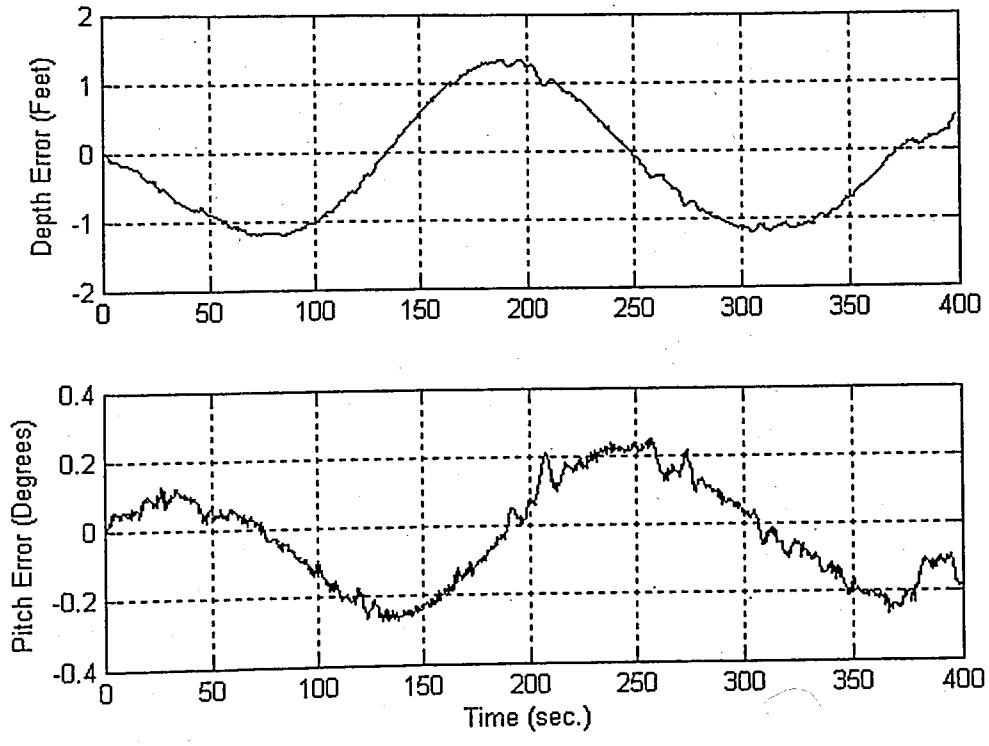

Figure 5.15. Depth and pitch error values for sea state 6 with modified equivalent control part of a sliding-mode controller [52]

5.2. Discussion

Two reconfiguring sliding mode controllers are proposed to compensate primarily the sea wave disturbances on the submarine..A state observer has obtained the disturbance information of sea waves or other disturbances caused by model mismatch on submarine dynamics. The first approach uses the extracted sea wave disturbance information in a way to update the corrective control part of a sliding-mode controller. This approach gives better result when compared with a standard sliding-mode controller that is designed by ignoring mentioned disturbances.

In fact the standard sliding-mode controller designed by ignoring the disturbances cannot cope with excessive environmental changes. Updating the controller using the disturbance information at the corrective control part modifies the sliding mode controller adaptively. Hence, the robustness of the controller is adjusted on-line and the overall performance of the controller is enhanced to overcome the disturbances caused by sea waves during shallow water operation.

On the other hand, the second approach uses the extracted sea wave disturbance information in a way to update the equivalent control part of a sliding-mode controller. This approach gives better result when compared with a standard sliding-mode controller and reconfiguring sliding-mode controller based on first approach. This can be seen clearly seen when the depth and pitch errors for sea state 6 depicted in Figure 5.15 for second approach namely, modified equivalent control part of a sliding-mode controller with the depth and pitch errors for sea state 6 depicted in Figures 5.2, 5.7 and 5.8 for standard sliding-mode controller and first approach, namely, switching gain sliding-mode controller.

However, second approach causes computational burden when compared with other two methods mentioned above. But, the computational burden cannot be considered a very important issue when the benefits of this approach for a high technology system.

Such approaches of reconfiguration are very useful for real case applications of this field. In return, a reconfiguring robust controller can be obtained in order to perform the tasks expected from a submarine. The simulations tested the applicability of the proposed

scheme on a large-scale submarine. However, the same controller scheme is a good candidate for autonomous underwater vehicles (AUV), which are required to operate accurately and reliably in harsh marine environment [54].

6. CONCLUSIONS

As the dynamic systems are becoming more and more complex, they require sophisticated controllers in order to achieve reliability task. Among these systems, underwater vehicles are commonly used for both commercial and military purposes.

Above all, the military applications of underwater vehicles are becoming more and more popular as there is a great need for NATO Navies to have unmanned underwater vehicles for mine hunting operations due to political reasons. Therefore, there is a great interest among research centers for designing autonomous underwater vehicles in order to operate independently. They are required to operate autonomously and continue their mission in case of excessive sea wave disturbances or faults. Also there is an increasing interest among NATO Navies to utilize autonomous underwater vehicles at shallow waters for harbor and port protection. This issue was one of the main issues of NATO mine warfare conference 2004 due to new perspective of highly valuable industrial target protection after 11^{th} September attacks of terrorists.

This dissertation aims to contribute this area of research. The proposed controller is aimed to reconfigure itself in an adaptive manner in case of environmental or fault effects. Autonomous underwater vehicles are under excessive environmental disturbance at shallow water operations and they need to have fault tolerant control systems in order to operate autonomously.

The basic idea in this dissertation is to design a controller using sliding-mode methodology, which can yield acceptable performance when uncertainties inserted into the process at any instant. The robustness against a fault or disturbance should be adjusted in such a way that the proposed sliding-mode controller should reconfigure the controller and adjust the robustness when a fault or disturbance is detected in the system dynamics.

The work presented in second chapter explains firstly the fault and failure terms, analytical redundancy concept together with residuals in order to detect faults. The fault

detection and isolation (FDI) design tools based on observers in order to provide the fundamentals to bound mentioned tools with extraction of fault or disturbance information is also introduced in this chapter. Residuals are generated by means of observers, which are robust to disturbances but sensitive to faults, which might occur in system, sensor or actuators. The same idea is used to extract fault or disturbance information. Case studies are also presented in this chapter with simulations on a SISO pneumatic servo valve and a MIMO linear system fault detection.

The fundamentals of sliding-mode controller method are described together with chattering phenomenon in third chapter. The relation between robustness and the magnitude of the controller gain vector is shown with a pneumatic servo valve model. The sliding-mode controller design for a pneumatic servo valve is simple with regard to only one fault is detected and there is only one corrective gain term that is pre-calculated. The corrective gain of the controller is switched to a greater value in order to compensate fault effects on system dynamics. Nevertheless, the main aim of this approach is to form a relation between reconfiguration of sliding-mode controller and fault or disturbance information. Therefore, a relation between fault or disturbance information and robustness of the controller is investigated.

Fault or disturbance information is extracted by means of observer based fault detection techniques and extracted fault or disturbance information is inserted into a MIMO linear system model sliding-mode controller for bias faults with two approaches. Firstly, the corrective gain vector of the sliding-mode controller is switched to extracted fault information when the fault is detected. The performance of proposed re-configuring sliding-mode controller based on switching of corrective gain vector with respect to extracted fault information is compared under the same fault condition with standard sliding-mode controller scheme.

The proposed scheme based on corrective gain vector re-configuration shows better performance than standard sliding-mode controller for the given case and stops system dynamics to wind-up, whereas the standard sliding-mode controller cannot cope with the faulty situation and causes system dynamics to wind-up.

The second approach for reconfiguring sliding-mode controller uses the extracted fault or disturbance information for the equivalent control part of the sliding-mode controller. This approach is implemented for the same MIMO system under the same faulty situation. It has been observed that the second approach gives better performance than the first one.

The proposed approaches are aimed to implement an autopilot for an underwater vehicle, parallel to the philosophy defined in first paragraph. Therefore, a submarine model is introduced in fourth chapter. The submarine model is explained for the depth and pitch angle control of the submarine with excessive sea wave effects at shallow submerged operation. The actuator model is also given with realistic physical constraints.

The reconfiguring sliding-mode controller concept with two approaches defined in third chapter is also implemented for the submarine model. The performance of three types of controllers is investigated. Standard sliding-mode controller designed for nominal plant shows poor performance and cannot cope with disturbances.

First approach based on inserting extracted disturbance information into corrective control part of standard sliding-mode controller shows better performance than a standard sliding-mode controller and perform shallow submerged depth control task. Second approach based on inserting extracted disturbance information into equivalent control part of sliding-mode controller shows better performance than the first one.

Therefore, proposed reconfiguring sliding-mode controller approaches have considerable advantages when compared with passive robust control reconfiguration controllers. They combine fault detection and isolation methods with sliding-mode controller scheme in an adaptive manner. The robustness of sliding-mode controller is updated in a way to compensate fault or disturbance effects. Hence, the proposed reconfiguring fault and disturbance tolerant controller that uses standard sliding-mode controller as the base-line controller is a good candidate to be implemented for underwater vehicles.

It is also Turkish Navy's interest as a NATO member country Navy to have autonomous underwater vehicles. So far, remotely operated vehicles are used on board mine hunting vehicles. It is planned to have national technological capability for underwater vehicles which will be the main factor of upcoming unmanned wars. Therefore, it is aimed to implement proposed approach for a national developed underwater vehicle for littoral water mine hunting operations and harbor and port protection tasks in future. Future work as the first step involves the development of a remotely operated vehicle and implementation of the proposed approach on this developed underwater vehicle. Next step will be going one step further, and having an autonomous underwater vehicle which will operate autonomously.

APPENDIX A: HYDRODYNAMIC COEFFICIENTS

The hydrodynamic coefficients and variables below are used in (2.2.) and (2.3).

Normal Force

$$Z'_w = -0.0110 \quad Z'_{\dot{w}} = -0.0075 \quad Z'_{\dot{\theta}} = -0.0045$$
$$Z'_{\ddot{\theta}} = -0.0002 \quad Z'_{\delta B} = -0.0025 \quad Z'_{\delta S} = -0.0050$$

Pitching Moment

$$M'_w = 0.0030 \quad M'_{\dot{w}} = -0.0002 \quad M'_{\dot{\theta}} = -0.0025$$
$$M'_{\ddot{\theta}} = -0.0004 \quad M'_{\delta B} = 0.0005 \quad M'_{\delta S} = -0.0025$$
$$I'_y = 5.6867 \times 10^{-4}$$

Sea Wave Forces

$$C_{M1} = 0.35 \quad C_{Z1} = 1.28 \quad C_{Z2} = 0.77$$
$$L = 286 Ft. \quad \nabla = 7.6 \times 10^4 Ft^3 \quad \rho = 2.0 slugs/Ft^3$$
$$U = 8.43 Ft/\text{sec}.$$

APPENDIX B: VECTOR NORMS

Definition:

The norm of a vector can be defined as a measure of the magnitude of that vector. Vector norms are used in (3.19) and (4.36) in this thesis.,

Let $\mathbf{x} = \begin{bmatrix} x_1 \\ x_2 \\ \vdots \\ x_n \end{bmatrix} \in R^n$. The Euclidean norm (or l_2) of $\mathbf{x}$ is defined by,

$$\|\mathbf{x}\| = \sqrt{x_1^2 + x_2^2 + \ldots + x_n^2}$$

Properties of Vector Norms

$$\|\mathbf{x}\| \geq 0,$$
$$\|\mathbf{x}\| = 0, \text{if and only if } \mathbf{x} = 0,$$
$$\|c\mathbf{x}\| = |c|\|\mathbf{x}\| \text{ for any scalar } c,$$
$$\|\mathbf{x} + \mathbf{y}\| \leq \|\mathbf{x}\| + \|\mathbf{y}\|.$$

As defined above, there is Euclidean or l_2 norm, there exists also; l_1 norm,

$$\|\mathbf{x}\|_1 = |x_1| + |x_2| + |x_3| + \ldots + |x_n|$$

l_∞ norm is defined as follows,

$$\|\mathbf{x}\|_\infty = \max\{|x_1|, |x_2|, |x_3|, \ldots, |x_n|\}$$

The norm defined in (3.19) and (4.36) are Euclidean vector norms.

REFERENCES

1. Van der Molen, G. M., and M. J. Grimble, "H_∞ Submarine Depth and Pitch Control," *Proc.IEEE Conference on Decision and Control*, Texas, USA, pp. 2511-2516, December 1993.

2. Dumlu, D., and Y. Istefanopulos, "Design of an Adaptive Controller for Submersibles via Multimodel Gain Scheduling," *Ocean Engineering*, Vol. 22, pp. 593-614, 1995.

3. Slotine, J. E., and W. P. Li, *Applied Nonlinear Control,* Prentice-Hall, 1991.

4. Yoerger, D. R., J. B. Newman, and J. E. Slotine, "Supervisory Control for the Jason ROV," *IEEE Journal of Oceanic Engineering*, Vol. OE-11, No.3, pp. 392-399, July 1986.

5. Cristi, R., F. A. Papoulias, and A. J. Healey, "Adaptive Sliding Mode Control of Autonomous Underwater Vehicles in the Dive Plane," *IEEE J. Oceanic Engineering*, Vol. OE-15, No. 3, pp. 152-160, July 1990.

6. Aström, K. J., and B. Wittenmark, *Adaptive Control*, Addison-Wesley, 1995.

7. Healey, A. J., and D. Lienard, "Multivariable Sliding Mode Control for Autonomous Diving and Steering of Unmanned Underwater Vehicles," *IEEE J. Oceanic Engineering*, Vol. OE-18, No. 3, pp. 327-338, July 1993.

8. Rauch, H. E., "Autonomous Control Reconfiguration," *IEEE Control System Magazine*, December 1995.

9. Blanke, M., "Fault Tolerant Control Systems," in P. M. Frank (ed), *Advance in Control*, pp. 171-196, 1999.

10. Singh, J., "Battlespace Access Unmanned Underwater Vehicles (BAUUV)," *Proc. Guidance and Control of Underwater Vehicles 03*, Newport, UK, pp. 3-4, 2003.

11. Huzmezan, M., *Reconfigurable Flight Control Methods and Related Issues, A Survey*, DERA Report No: ASF/3455, Sep. 1997.

12. Keating, M. S., M. Pachtet, and C. H. Houpis, "QFT Applied to Fault Tolerant Flight Control System Design," *Proc. Automatic Control Conference 95*, Seattle, USA, June 1995.

13. Murad, G. A., I. Postletwaite, and D. W. Gu, "A Robust Design Approach to Integrated Controls and Diagnostics," *Proc. 13th IFAC World Congress*, San Francisco, June 1996.

14. Moerder, D. D., N. Halyo, J. R. Broussard, and A. K. Cağlayan, "Applications of Pre-Computed Control Laws in a Reconfigurable Aircraft Flight Control System," *Journal of Guidance, Control and Dynamics*, Vol. 13(6), 1990.

15. Ostroff, A., "Techniques for Accommodating Control Effector Failures on Mildly Statically Unstable Airplane," *Proc. Automatic Control Conference 85*, 906-913, 1985.

16. Morse, W. D., and K. A. Ossman, "Model Following Reconfigurable Flight Control System for the AFTI/F-16," *Journal of Guidance, Control and Dynamics*, Vol. 13(6), 1990.

17. Groszkiewicz, J. E., and M. Bodson, "Flight Control Reconfiguration Using Adaptive Methods," *Proc. 34th Conference on Decision and Control*, pp. 1159-1164, New Orleans, LA, USA, 1995.

18. Bodson, M., "Multivariable Adaptive Algorithms for Reconfigurable Control," *IEEE Trans. on Control Systems Technology*, Vol. 7(2), pp. 217-227., March 1997.

19. Demirci, U., and F. Kerestecioğlu, "Active Reconfigurable Control of a Submarine with Indirect Adaptive Control," *Proc. Oceans 03*, No. 616, San Diego, USA, 2003.

20. Chen, J., and R. J. Patton, *Robust Model-Based Fault Diagnosis for Dynamic Systems*, Kluver Academic Publishers, 1999.

21. Isermann, R., "Supervision, Fault-Detection and Fault-Diagnosis Methods – An Introduction," *Control Engineering Practice*, Vol. 5, pp. 639-652, 1997.

22. Frank, P. M., "Fault Diagnosis in Dynamic System Using Analytical and Knowledge Based Redundancy," *Automatica*, Vol. 26(3), pp. 459-474, 1990.

23. Gertler, J., "Fault Detection and Isolation Using Parity Relations," *Control Engineering Practice*, Vol. 5, No. 5, pp. 653-661, 1997.

24. Leonhardt, S., and M. Ayoubi, "Methods of Fault Diagnosis," *Control Engineering Practice*, Vol. 5, No. 5, pp. 683-692, 1997.

25. Willsky, A. S., "A Survey of Design Methods for Failure Detection in dynamic Systems" *Automatica*, Vol. 12, pp. 601-611, 1976.

26. Khalil, H. K., *Nonlinear Systems*, Prentice Hall, Englewood Cliffs, NJ, 2002.

27. McGookin, E. M., "Fault Tolerant Sliding Mode Control for Submarine Manoeuvring," Proc. *1st IFAC Workshop on Guidance and Control of Underwater Vehicles 03*, Newport, South Wales, UK, pp. 119-124, 2003.

28 Yen , G. G., and L. W. Ho, "Fault Tolerant Control: An Intelligent Sliding Mode Control Strategy," *Proc. Automatic Control Conference 00*, pp. 4204-4208., Chicago, Illinois, USA, June 2000.

29. Patton, R. J., "Fault-Tolerant Control Systems: The 1997 Situation," *Proceedings SAFEPROCESS 97*, Hull, UK, pp. 1033-1054, 1997.

30. Fossen,T. I., *Guidance and Control of Ocean Vehicles*, John Wiley & Sons, NY, 1994.

31. Burcher R., and L. Rydill, *Concepts in Submarine Design*, Cambridge Ocean Technology Series, Cambridge University Press, 1998.

32. Richards, R. J., and D. P. Stoten, "Depth Control of a Submersible Vehicle," *Int. Shipbuilding Progr.*, Vol 29, No.326, pp. 30-40, 1982.

33. Price, W. G., and R. E. D., Bishop, *Probabilistic Theory of Ship Dynamics*, Chapman and Hall, London, 1974.

34. Mandzuka, S., "Mathematical Model of a Submarine Dynamics at the Periscope Depth," *Brodogradnja*, Vol. 36, pp. 5-6, 1998.

35. Borgman, L. E., "Ocean Wave Simulation for Engineering Design," *Journal of Waterways and Harbours Division*, ASCE, WW4, pp. 557-583, 1969.

36. Gran, S., "A Course in Ocean Engineering," *Developments in Marine Technology*, No. 8, Elsevier Science Publishers B. V., 1992.

37. Clark, R. N., P. M. Frank, and R. J. Patton, M.J. Grimble (Ed.), *Fault Diagnosis in Dynamic Systems*, Prentice Hall, 1989.

38. Clark, R. N., D. C. Fosth and W.M. Walton, "Detecting Instrument Malfunctions in Control Systems," *IEEE Transactions on Aerospace and Electronic Systems*, Vol. AES-11 No.4, pp. 465-473, 1975.

39. Montgomery, R. C., and A. K. Çağlayan, "Failure Accommodation in Digital Flight Control Systems by Bayesian Decision Theory," *Journal of Aircraft*, Vol. 13(2), pp. 69-75, 1976.

40. Deckert, J. C., M. N. Dessai, J. J. Deyst, and A. S. Willsky, "F-8 DFBW Sensor Failure Identification Using Analytic Redundancy," *IEEE Trans. Automatic Control*, Vol. AC-22(5), pp. 795-803, 1977.

41. Fuente, M. J., P. Vega, M. Zarrop, and M. Poch, "Fault Detection in a Real Wastewater Plant Using Parameter Estimation Techniques, *Control Eng. Practice*, Vol. 4, No. 8, pp. 1089-1098, 1996.

42. Wünnenberg, J. and P. M. Frank, "Sensor Fault Using Detection via Robust Observers," Tzafestas, S. G., M. G. Singh, and G. Schmidt (Eds.), *System Fault Diagnostics, Reliability and Related Knowledge-based Approaches*, D. Reidel Press, pp. 147-160, 1987.

43. Demirci, U., and F. Kerestecioğlu, "Reconfiguring Sliding Mode Controller for a Pneumatic Servo mechanism," *Proc. Underwater Defence Technology Conference 02*, PI-16, LaSpezia, Italy, 2002.

44. Ho, G. H., and C. L. Teo, "Position Control of a Pneumatic Servo Mechanism," *Recent Advances in Mechatronics,* pp. 372-386, Springer, Singapore, 1999.

45. Hamiti, K., A. Voda-Besançon, and H. Roux-Buisson, "Position Control of a Pneumatic Actuator under the Influence of Stiction," *Cont. Eng. Practice,* Vol. 4, pp. 1079-1088, 1996.

46. Ogata, K., *Modern Control Engineering*, Prentice Hall, New Jersey, 2002.

47. Demirci, U., and F. Kerestecioğlu, "Fault-Tolerant Reconfiguring Sliding Mode Controller", submitted to *Elektrik: Turkish Journal of Electrical Engineering and Computer Sciences*, 2004.

48. Demirci, U., and F. Kerestecioğlu, "Fault-Tolerant Reconfiguring Sliding Mode Controller", *Proc. ELECO 03 Conference*, Bursa, pp. 279-283, 2003.

49. Young, D. K., V. I. Utkin, and Ü. Özgüner, "A Control Engineer's Guide to Sliding Mode Control," *IEEE Trans. Control Systems Technology*, Vol. 7, No. 3, pp. 328-342, May 1999.

50. Slotine, J. E., "Sliding Controller Design for Nonlinear Systems," *Int. J. Control*, Vol. 40, No. 2, pp. 421-434, 1984.

51. Demirci, U., and F. Kerestecioğlu, "Sliding Mode Controller Solution for the Shallow Submerged Operation of a Submarine," *Proc. Guidance and Control of Underwater Vehicles 03*, Newport, UK, pp. 113-117, 2003.

52. Demirci, U., and F. Kerestecioğlu, "A Reconfiguring Sliding Mode Controller with Adjustable Robustness," accepted for publication by *Ocean Engineering*, 05 January 2004.

53. Edwards, C., Spurgeon, S. K., *Sliding Mode Control Theory and Applications*, Taylor and Francis, 1998.

54. Lapierre, L., D. Soetanto, and A. Pascoal, "Nonlinear Path Following Control of Autonomous Underwater Vehicles," *Proc. Guidance and Control of Underwater Vehicles 03*, Newport, UK, pp. 29-34, 2003.

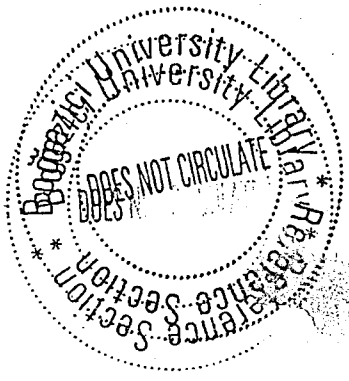
Boston University Library
Reference Section
DOES NOT CIRCULATE